THE EFFECT OF DOLERITE INTRUSIONS ON THE HYDROCARBON POTENTIAL OF THE LOWER PERMIAN WHITEHILL FORMATION (KAROO SUPERGROUP) IN SOUTH AFRICA AND SOUTHERN NAMIBIA: A PRELIMINARY STUDY

T. SMITHARD, E.M. BORDY AND D. REID
Department of Geological Sciences, University of Cape Town, Private Bag X3,. Rondebosch, 7701. Cape Town, South Africa
e-mail: travis.smithard@gmail.com; emese.bordy@uct.ac.za; david.reid@uct.ac.za

ABSTRACT

Recent interest in the shale gas potential in the main Karoo Basin of South Africa has focused attention mainly on the carbonaceous Whitehill Formation (Ecca Group, Karoo Supergroup). To unravel the metamorphic effect of the Lower Jurassic Karoo igneous intrusions on the Lower Permian Whitehill Formation, outcrop samples were taken at various distances (ranging from 1 to >30 m) from the intrusive contacts of dolerite sills in the western part of the main Karoo Basin (Northern Cape, South Africa) and in the Karasburg Basin (southern Namibia). Furthermore, to establish the baseline petrological and geochemical composition of the Whitehill Formation, samples have also been collected at localities unaffected by dolerites in the southern main Karoo Basin. Mineral assemblages from all sample localities plot within the chlorite zone and show very low grade metamorphism. Mineral assemblages and illite crystallinity data indicate that the Whitehill Formation has undergone (a) anchizone metamorphism (250 to 300°C) in the southern main Karoo basin as well as in areas close to the dolerite intrusions, and (b) moderate burial diagenesis (~180°C) in areas away from the immediate effect of dolerites in the Northern Cape and southern Namibia. Regional evaluation of unconventional gas potential of the Karoo basins of southern Africa ought, therefore, to consider the subsurface thickness and spacing of Karoo intrusive bodies within the target carbonaceous formations.

Introduction

Heightened global interest in the exploitation of unconventional gas resources has concentrated geoscientific attention on the understanding of the evolution of carbon-based energy resources within the Karoo basins of southern Africa (De Wit, 2011; Maré et al., 2014; Scheiber-Enslin et al., 2014). Apart from the Permian Karoo coal deposits, the highest total organic carbon (TOC) content is found in the 280 ± 2.1 Ma old, Lower Permian Whitehill Formation (Figures 1; 2), which comprises laminated carbonaceous mudstones (siltstones and claystones). Previous authors (e.g., Rowsell and de Swardt, 1976; Anderson and McLachlan, 1979; Cole and McLachlan, 1991) suggested that due to the high degree of burial diagenesis in the southern part of the region and the adverse effects of Early Jurassic (183 ± 1 Ma - Duncan et al., 1997) Karoo igneous intrusions, the conventional oil and gas within the Karoo basins had low economic potential at the time of their studies. With the exception of a few recent studies (cf. Maré et al., 2014; Scheiber-Enslin et al., 2014 and summaries therein), the impact of the dolerite intrusions on the unconventional gas potential of the Karoo Basin remains poorly researched. Generally, the effect of thermal stress on the country rocks by an intruding magma is variable, and estimates on the width of the thermal aureole range from twice the thickness to less than half the thickness of the intrusive body (Dow, 1977; Raymond and Murchison, 1988; Krynauw et al., 1994; Golab and Carr, 2004; Bussio, 2012). The variability in estimating the size of the thermally altered zone is attributed to the variability in the thermal conductivities of country rocks, rates of heat transfer, the effects of dehydration and evaporation reactions in reducing the heat energy balance, as well as the degree of organic matter maturation prior to igneous intrusions (Galushkin, 1997; Wang, 2012; Bussio, 2012). Currently, the literature is limited on the unconventional dry-gas potential of highly mature shale reservoirs. Although Price (1995), pointed out that significant unconventional dry-gas resources within over-mature (R_0 >4%) carbonaceous shales, albeit uncommon, do exist (e.g., Sacramento and West Texas Permian Val Verde Basins), this study pre-dates the significant expansion of shale gas production in the 2000s, and the commercial prospectivity of such deposits. Indeed, based on the current shale gas exploration experience, which is still mostly limited to North America, it has been suggested that commercial production is economically unviable at R_0 maturities greater than 3.5% (e.g., Zagorski et al., 2012). Furthermore, Laughrey et al. (2011) showed that at graphite facies metamorphism (R_0 = 4%), kerogen-to-graphite conversion and authigenic mineral overgroweighths (as well as structural deformation) may well destroy the porosity and self-sealing capacity of shale reservoirs.

The objective of this study is to identify the thermal maturation effects of diagenesis and contact

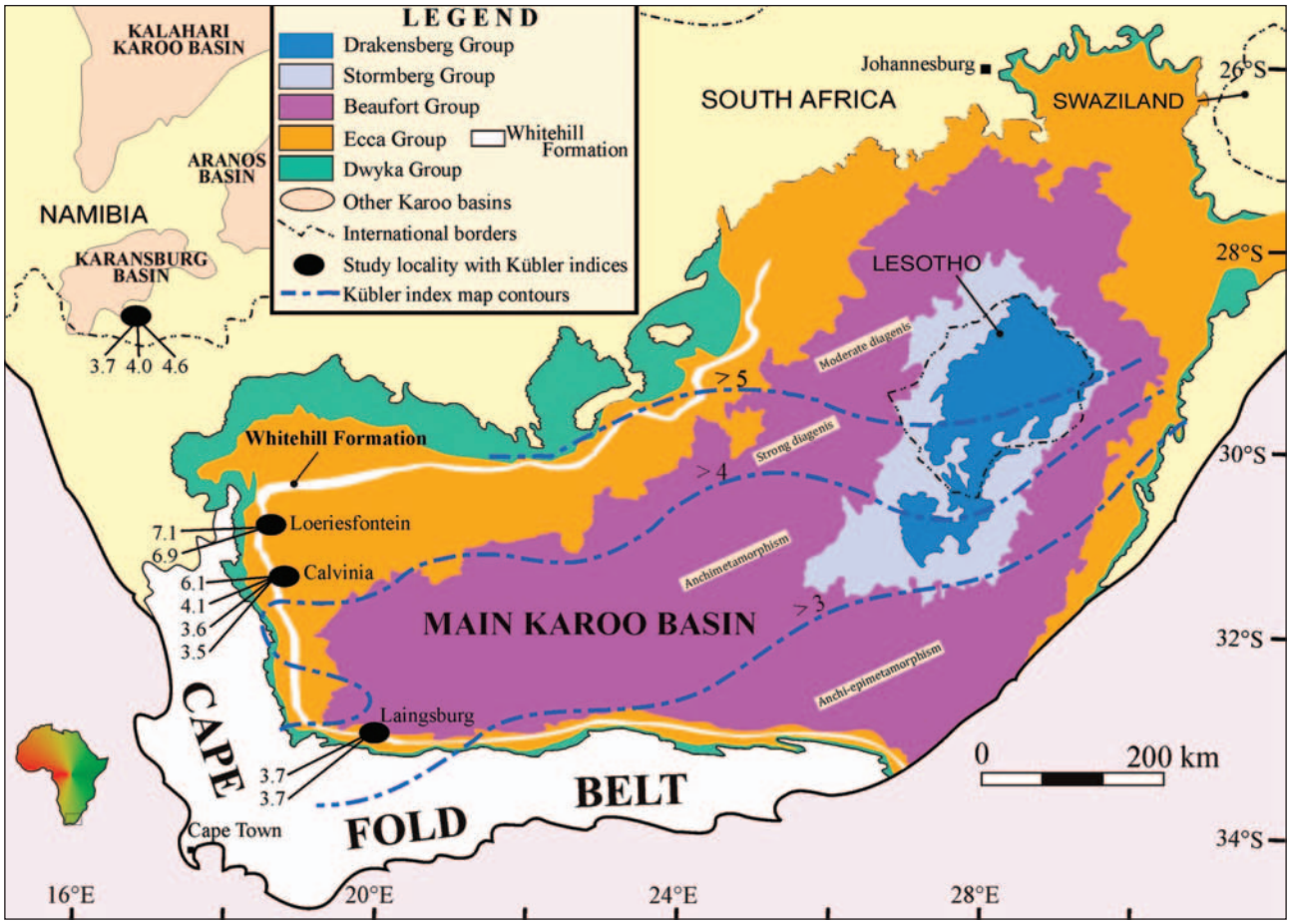

Figure 1. *General geological map of South Africa, showing the extent of the main Karoo Basin. The Early Permian Whitehill Formation crops out extensively along the southern and western portions of the basin as well as in the Karasburg Basin (southern Namibia). The blue dashed lines show the Kübler Index (expressed as 10 x Δ°2Θ) contours within the main Karoo Basin Map modified after Rowsell and de Swardt (1976) and Johnson et al. (1996).*

metamorphism by Jurassic dolerite intrusions on the carbonaceous Permian Whitehill Formation based on relatively fresh outcrop samples taken at variable distances from dolerite intrusive contacts in western South Africa and southern Namibia (Figure 1). Using routine geological and analytical methods (e.g., petrography, XRD, XRF, illite crystallinity), the study also aims to assist in assessing the unconventional hydrocarbon potential of the Lower Permian Whitehill Formation.

Geological background

The Whitehill Formation is contained in the lower part of the Permian Ecca Group, which forms part of the Late Carboniferous-Early Jurassic Karoo Supergroup, and is exposed in the study areas in western South Africa and southern Namibia (Figures 1; 2). The lower Ecca Group in this region (Figure 2) is a succession of conformable, mainly argillaceous sedimentary rocks that were deposited initially in a deep water setting characterized by pelagic and mass movement sedimentation (Johnson, 1976; Visser and Loock, 1978; Kingsley, 1985; Cole and Basson, 1991; Cole, 1992; Visser, 1993; Faure and Cole, 1999; Rubidge et al., 2000; Werner, 2006). This initial deeper water phase was followed by the gradual shallowing of the basin which resulted in sedimentation on and near an open shelf and eventually shoreface settings and deltas (ibid.). The formations of the lower Ecca Group, namely the Prince Albert, Whitehill and Collingham formations (Figure 2A) have consistent lithologies throughout the study area and are thus unambiguously traceable from southern Namibia to Laingsburg in the southern main Karoo Basin (Cole, 1992).

The difference in tectonic styles between the main Karoo Basin and the Karoo basins in Namibia is noted by Catuneanu et al. (1998) and Stollhofen et al. (2000). These studies show that during the Dwyka and lower Ecca deposition, the Karoo basins of Namibia formed under extension and are associated with rift basin subsidence, whilst the main Karoo Basin in South Africa formed under compression and is associated with mainly flexural subsidence, characteristic of foreland basins, although the tectonic setting of the basin remains debated (cf. Tankard et al., 2012; recent summary in Scheiber-Enslin et al., 2014). These basin-forming

tectonic processes, together with regional climate changes that resulted in the melting of the Permo-Carboniferous ice caps, generated the accommodation space of the Mesosaurus Inland Sea, which apparently covered the southern portion of Gondwana at the time (Figure 2B) (Stollhofen et al., 2000; Werner, 2006).

The Whitehill Formation

The white-weathering Whitehill Formation is distinguished at outcrop-scale from the dark grey-coloured lithologies in the underlying Prince Albert Formation and overlying Collingham Formation (Figure 2A) (Anderson and McLachlan, 1979). The Whitehill Formation consists of pyritic, thinly laminated carbonaceous shales (Figure 3A) that show variation in silt content both laterally and vertically at various scales, leading to the difference in weathering colour and hardness (Figures 3B to E) (Cole and Basson, 1991). The Formation is also known for its ubiquitous diagenetic carbonate, chert and phosphatic concretions, which vary from spherical and ellipsoidal to tube-like bodies within the shales (Figure 3F, G, H) (ibid.). In weathered outcrops, the carbonaceous shales of the Formation often, but now always, appear white (especially from a distance) due to the diagenetic alteration of the locally high sulphur (pyrite) content to sulphates (e.g., gypsum) (ibid.).

Based on sedimentological and paleontological evidence, the fine-grained, fissile, carbonaceous shales in the Whitehill Formation accumulated in a few million years within the low-energy, stratified, deep-water body of the Mesosaurus Inland Sea of southwestern Gondwana (Figure 2B) (Oelofsen, 1981; Cole and McLachan, 1991; Visser, 1992; 1993). Within this stratified water-body, the oxygenated surface waters enabled primary productivity of planktonic algae, whereas the reducing bottom waters preserved the organic material received by the basin (plankton, land-derived *Glossopteris* leaves, pollen, spores, etc.) (ibid.). Biogeochemical transformations, through geological time, ultimately resulted in the reported total organic carbon (TOC) content of the Whitehill Formation which ranges locally from 0.5 to 17% (average TOC: ~4.5%; e.g., Oelofsen, 1987, p. 132; Cole and McLachlan, 1991, p. 104).

The Formation shows lateral thickness variation within the main Karoo Basin from a maximum of 80 m thickness in the southwest to an average of 15 m thickness in the northeast, and its northeastern limit runs roughly parallel to a line south of the southwestern border of Lesotho with South Africa (Figure 1) (Anderson and McLachlan, 1979; Cole and McLachlan, 1991). In Namibia, the thickness of the Formation decreases in a northerly direction from 40 m thick in the Karasburg Basin to approximately 8 m thick in the Aranos Basin (Figure 1) (Werner, 2006). Body and trace fossil assemblages of the Whitehill Formation permitted the biostratigraphic subdivision of the unit in South Africa (Oelofsen, 1987), and assisted in the detailed reconstruction of the Early Permian palaeo-environments and regional correlations in southwest Gondwana (Figure 2B). Among others, Oelofsen's (1981; 1987) vertical fossil zonation within the Whitehill Formation suggests fluctuations in oxygen and salinity

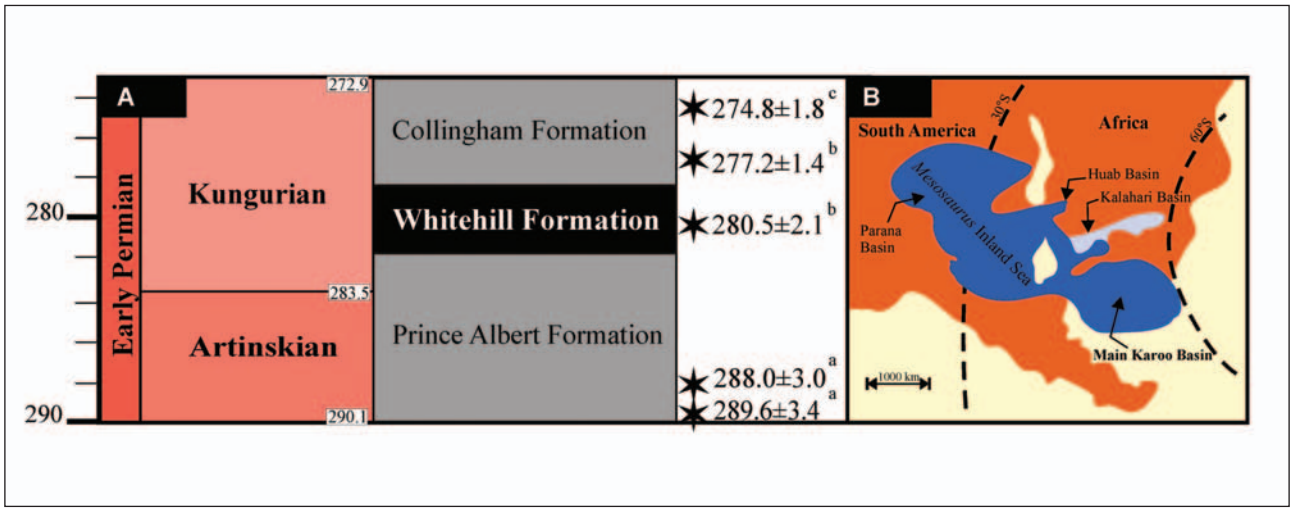

Figure 2. *(**A**) The chronostratigraphy of the Lower Permian Ecca Group (Karoo Supergroup) in the southern main Karoo Basin and Namibia (modified after Rubidge, 2005). Radiometric dates are marked with black stars, shown in million years and taken from **a**: Bangert et al., 1999; **b**: Werner, 2006; **c**: Fildani et al., 2007. Geological time scale based on 2013 ICS Time Chart. (**B**) Palaeogeographic map of southwest Gondwana in the Early Permian and the approximate extent of the Mesosaurus Inland Sea (in blue) in which the Whitehill Formation and its correlatives accumulated (e.g., Irati Formation of Brazil; Mangrullo Formation of Uruguay; the upper part of the Tubarão Formation and the Tacaury Formation of Paraguay, the Black Rock member of the Falkland Islands and the upper part of the Vryheid Formation in the northeastern part of the main Karoo Basin – Oelofsen and Araújo, 1983; Visser, 1992, 1993; López-Gamundi et al., 1995; Johnson et al., 1997; Werner, 2006). Map modified after Faure and Cole (1999) and Werner (2006).*

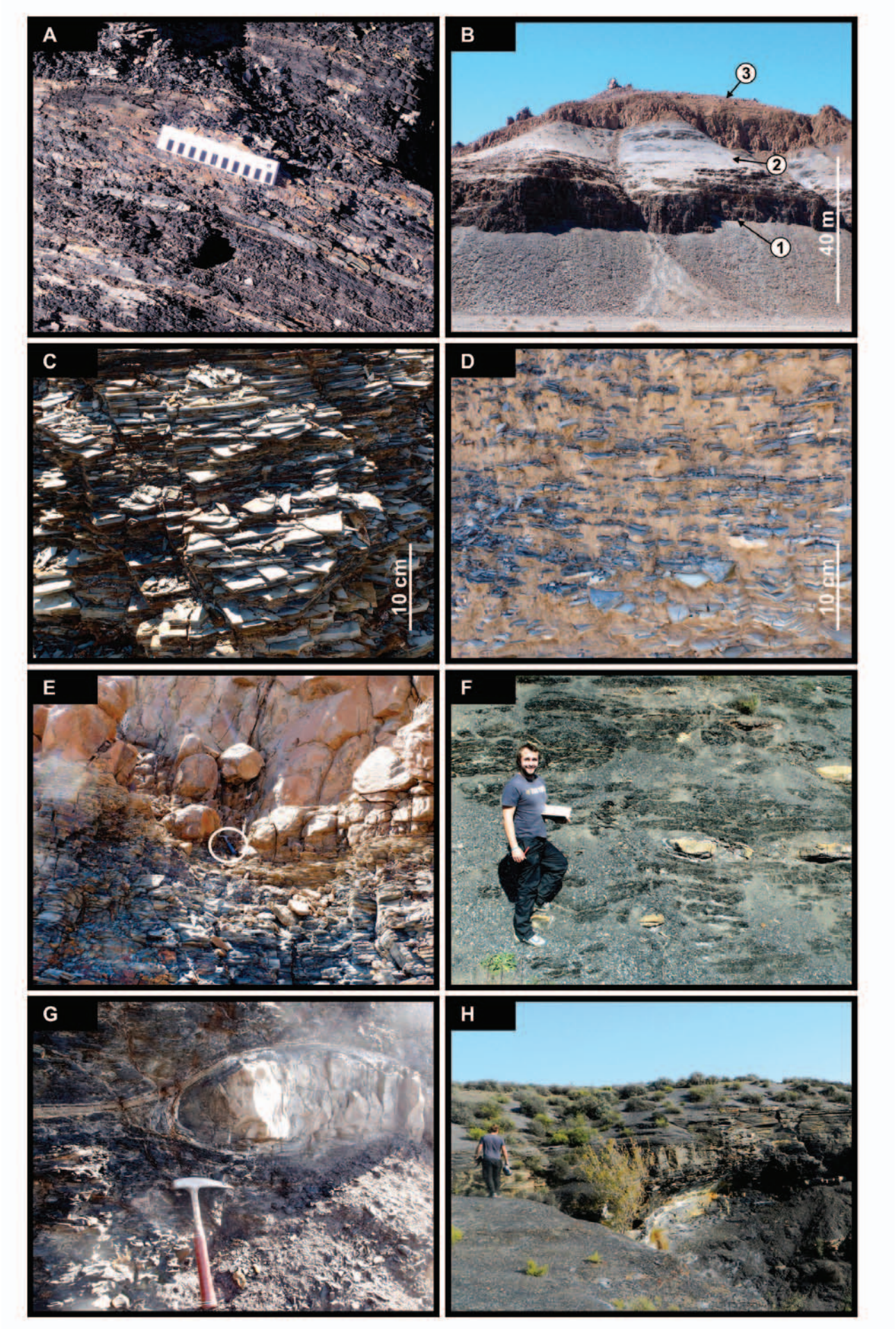
A
B
3
2
1
40 m
C
10 cm
D
10 cm
E
F
G
H

Figure 3. *(**A**) The Whitehill Formation near Laingsburg (Western Cape, South Africa) comprises very thinly bedded to laminated carbonaceous shales. (**B**) Whitehill Formation (1 and 2) intruded by a Karoo dolerite sill (3) in the Karasburg Basin (southern Namibia). The Formation here displays two characteristic zones: a lower, brown-green weathering shale zone with higher silt content (1) and cliff-forming habit (see close-up in **C**), and an upper, less resistant. white to bluish-grey weathering shale zone (2; see close-up in **D**). (**E**). Details of the intrusive contact between the Whitehill Formation and the sill (hammer for scale in white circle). (**F**) Diagenetic carbonate concretions are variable in shape (see close-up in **G**) and size, and abundant within the middle part of the Whitehill Formation in the Loeriesfontein region (Northern Cape, South Africa). (**H**) Weathering of the localized, high sulphur content in the Whitehill Formation leads to characteristic white and light yellow patches that contrast against the black carbonaceous shales.*

levels, implying that the original distribution of the organic matter in the sediments was also variable both through time and space. Such changes in the syn-sedimentary physico-chemical conditions have been subsequently confirmed quantitatively by various localized geochemical analyses (e.g., trace element and chemical index of alteration studies – Cole and McLachan, 1991; Faure and Cole, 1999; Rimmer, 2004; Scheffler et al., 2006; Werner, 2006). Although, Visser (1992) presented a lithofacies correlation of the Whitehill Formation across the basin and proposed a boundary between the facies of shallow and deeper water settings, systematic mapping of the compositional changes (mineralogy, geochemistry, organic content, etc.), within the Whitehill Formation has not yet been undertaken on a basinal scale.

Karoo dolerites

Lower Jurassic fine- or medium-grained mafic intrusions (i.e., Karoo dolerites) are prolific throughout the Karoo Supergroup and caused the compartmentalization, fracturing and thermal alteration of the subsurface geology especially in the post-Ecca successions (e.g., Chevallier and Woodford, 1999; Chevallier et al. 2001; Maré et al., 2014; Scheiber-Enslin et al., 2014; Senger et al., 2015). The individual dolerite intrusions have been proposed to have composite geometries with mostly irregular spacing by regional, low resolution or very localized higher resolution geological and geophysical studies (e.g., Cole and McLachlan, 1991; Chevallier and Woodford, 1999; Chevallier et al., 2001; Scheiber-Enslin et al., 2014; Senger et al., 2015). It is noteworthy that to date, systematic, high resolution subsurface studies of these Karoo dolerites are non-existent in the western main Karoo Basin. For this part of the Basin, data analysis by Svensen et al. (2015, their Figure 7B) of a few Karoo drill cores shows that ~50% of the dolerite sills are less than 30 m thick. Furthermore, Svensen et al. (2015, their Figures 5 and 7B) also suggests that most (~80%) of the sills in the Ecca Group are less than 30 meters thick and widely spaced (>100 m) in this region of the Karoo Basin.

Based on recent U-Pb zircon (and baddeleyite) dating, Karoo sills have over-lapping ages of 183.0 ± 0.5 Ma and 182.3 ± 0.6 Ma (Svensen et al., 2012). These coherent ages are concordant with the widely cited and accepted date of 183 ± 1 Ma for the Karoo Igneous Event (Duncan et al., 1997) and supports the very rapid emplacement rate of the Karoo magmas suggested by earlier authors (e.g., Duncan et al., 1997; Marsh et al., 1997). Corroborated by magneto- and geochemical stratigraphies, the rapid emplacement rate of 0.78 km^3/yr indicates that the estimated volume of magma (367 000 km^3) could have been emplaced in 0.47 million years (Hargraves et al., 1997; Marsh et al., 1997; Svensen et al., 2012).

Methodology

A total of 15 pelitic rock samples were collected from outcrops of the Whitehill Formation in western part of South Africa and southern Namibia, at distances ranging from 1 to well over 30 m from the contact with dolerites (Figures 1, 4; Appendix 1). To constrain the mineralogy as well as textures of the shale samples, electron microprobe analyses and back-scatter electron imagery (BSE) were performed on polished thin sections. X-Ray Diffraction (XRD) was utilized for the identification of minerals as well as the crystallinity index of illite. X-Ray Fluorescence (XRF) was used for the determination of the major and trace elements in the samples. Furthermore, Bemlab laboratories (www.bemlab.co.za) analysed the total organic carbon (TOC) content of some selected samples. With the exception of the latter, all analytical procedures were conducted in the Department of Geological Sciences at University of Cape Town, and the full dataset on all the samples (e.g., GPS coordinates, mineralogy, XRF, XRD and illite crystallinity) is available in Appendix 1.

Results

Petrography

Authigenic metamorphic minerals in our Whitehill Formation samples were identified in the petrographic studies in conjunction with textural observations (Figures 5 to 8; Table 1; Appendix 1). These show that the massive to cross-laminated and horizontally-laminated sedimentary fabrics (e.g., Figures 7A and B; 8A), appear to be common in many of the samples, regardless of their position relative to the dolerites (Figure 5). However, samples that were closer than 1.5 m to the dolerites in the Karasburg Basin as well as sample 17 that was bounded by two dolerite sills near Calvinia are the exceptions to this, in that they displayed a distinctive crystalline texture. While most shale samples are horizontally laminated, indicating a low energy, quiet water settling from suspension, ripple

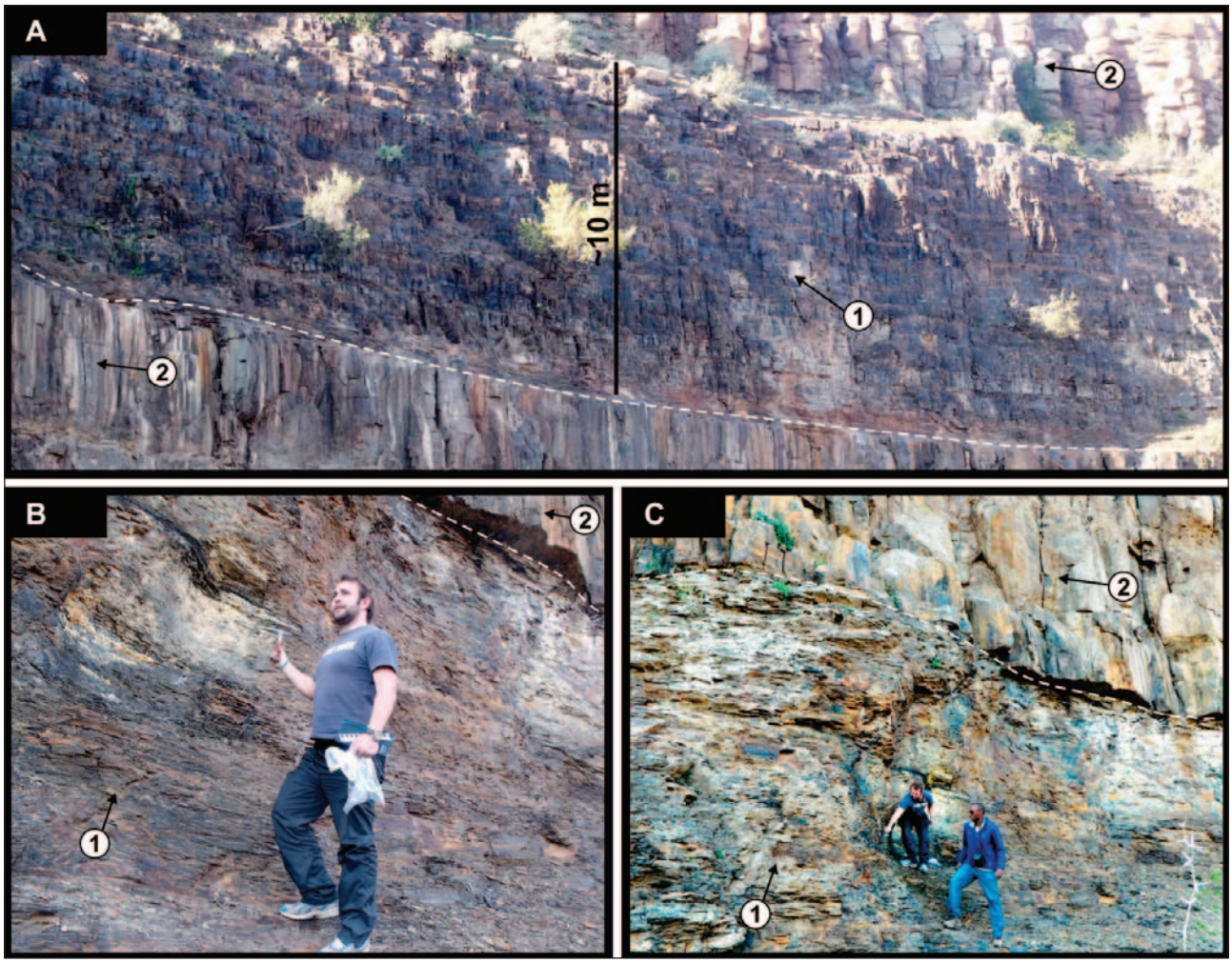

Figure 4. *Sampled outcrops near Calvinia (Northern Cape, South Africa) showing the highly variable fabric of the Whitehill Formation (1) adjacent to dolerite sills (2). (**A**) The pelitic rocks of the Whitehill Formation are usually harder and have a well-developed blocky jointing pattern between closely spaced dolerite sills. (**B**) Even in close proximity (<0.5 m) to dolerite sills, the Whitehill Formation may retain its distinctive black colour and primary lamination. (**C**) Alternatively, the highly mottled appearance suggests some form of thermal metamorphism.*

Figure 5. *Mineral assemblages of some of the Whitehill Formation samples taken at variable distances relative to dolerite sills. For details on the other samples, see Appendix 1.*

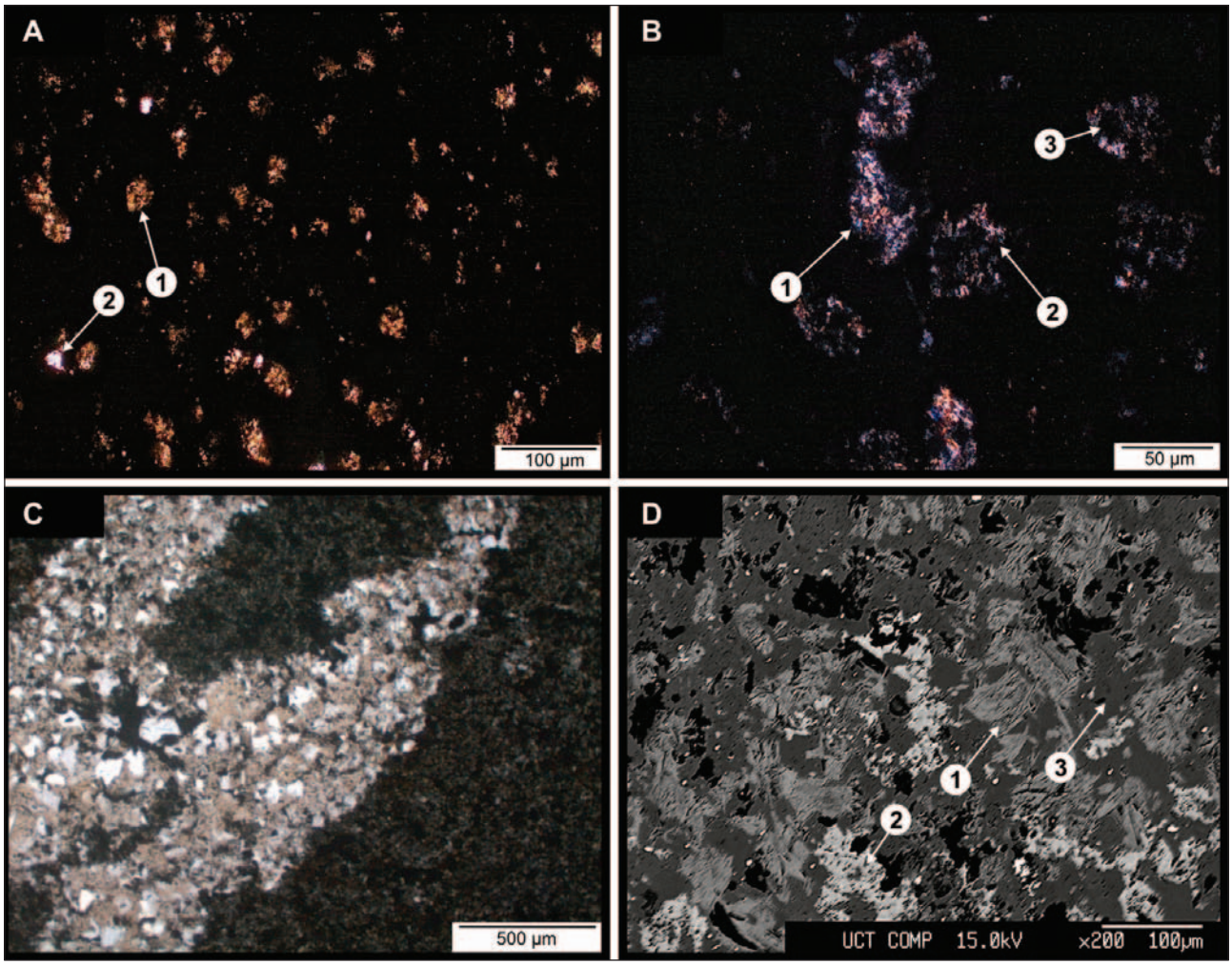

Figure 6. *Photomicrographs of Whitehill Formation samples taken <2.5 m away from a dolerite sill in the Karasburg Basin (southern Namibia). (**A**) Sub-rounded Na-K feldspar (1) and quartz (2) grains in sample 4, taken 2.5 m below sill (in cross-polarised light). (**B**) Highly birefringent white mica (1). alteration minerals (2) as well as the reaction rim around a feldspar (3) in sample 2 taken 1.5 m from sill (in cross-polarised light). (**C**) Vein containing quartz grains and a fine-grained matrix of muscovite and illite in a sample 3 taken 1 m below sill (in cross-polarised light). (**D**) Acicular (needle-like) groweighth of phengite over muscovite (1) in sample 3 also containing feldspar (2) and quartz (3) (back-scattered electron image). For location and other details of these samples, see Appendix 1.*

Table 1. Texture and mineral composition of Whitehill Formation samples based on optical microscopy and XRD results (for details, see Figures 5 to 8; Appendix 1). Dolerite sills do not occur at the Loeriesfontein study locality, thus the samples are assumed to be affected by dolerites that are >30 m away from the sample sites. The samples from the Karasburg Basin and Calvinia are those that were taken <5 m from a dolerite contact. Samples from Laingsburg and Loeriesfontein are combined as these sites were both lacking any dolerite intrusions.

		Locality		
		Main Karoo Basin Northern Cape, South Africa		**Karasburg Basin Southern Namibia**
		Loeriesfontein/Laingsburg	***Calvinia***	
Grain size	Average	20 µm	50 µm	40 µm
	Range	10 to 30 µm	20 to 80 µm	30 to 60 µm
Mineral assemblages		Quartz, illite, chlorite*, muscovite*, Na-K feldspar, organic carbon	Quartz, illite, phengite, muscovite, albite, chlorite, calcite**	Quartz, illite, phengite, albite, muscovite
Textures		Sedimentary lamination due to grain size variation	Sedimentary lamination preserved in sample below the dolerite. Sample above the dolerite has a crystalline texture with growth weight of authigenic micas	Authigenic mica alteration of feldspar, crystalline texture proximal to dolerite

*detrital phyllosilicate **possible hydrothermal alteration mineral

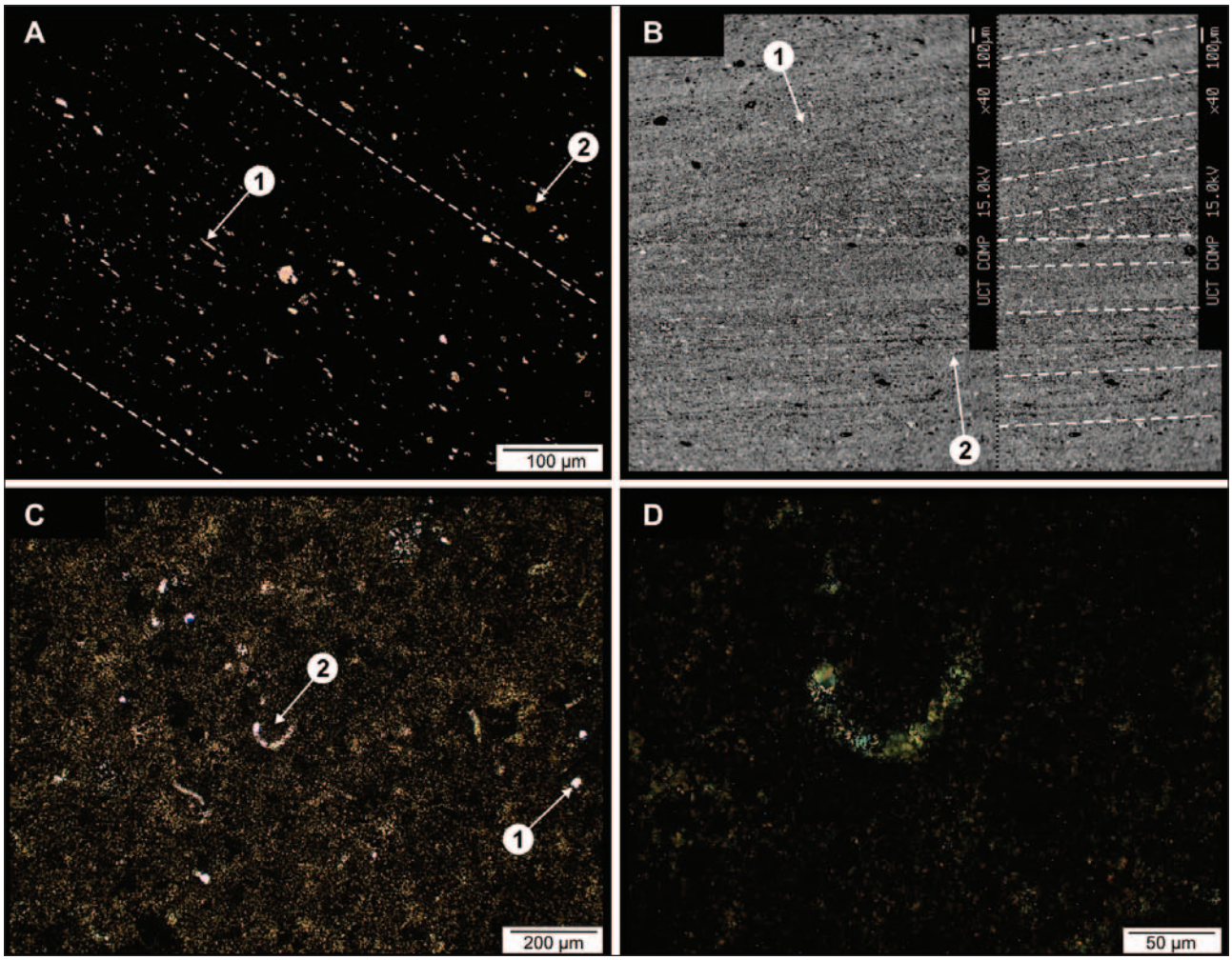

Figure 7. *Photomicrographs of the Whitehill Formation samples taken >30 m away from any dolerite sills near Loeriesfontein (Northern Cape, South Africa). (**A**) Sedimentary lamination (dashed lines) shown by lath-shaped detrital grains of mainly quartz (1) and mica (2) (in plane-polarised light; sample 11). (**B**) Highly carbonaceous, ripple cross-laminated (1) and horizontally-laminated (2) sandy siltstone (back-scattered electron image; sample 11). Part of the image has been duplicated at the right (hence the instrumental conditions label is repeated), so as to annotate the sedimentary structures. (**C**) Carbonaceous shale with quartz (1) and a possible shell fragment (2) (in plane-polarised light; sample 12). (**D**) close up of 2 in (C) (cross-polarised light). For location and other details of these samples, see Appendix 1.*

cross-laminated silty very fine sandstones (Figure 7B) suggests gentle currents over the depositional surface. The presence of such primary sedimentary features, even in samples taken <5 m from dolerites (e.g., samples 2, 4, 16), indicates that the pressures and temperatures in the study area were not uniformly sufficient to replace the primary sedimentary fabrics neither in the south, by deep burial diagenesis and tectonic deformation near the main fold-and-thrust zone of the Cape Fold Belt, nor in the north, due to contact metamorphism and moderate burial diagenesis. The presence of primary sedimentary fabric in our Laingsburg samples is consistent with accounts of other Ecca Group sedimentary units in the southern main Karoo Basin (e.g., Byrnes, 2013) which were shown by Frimmel et al. (2001) to have been exposed to lowermost greenschist facies conditions during the formation of the Cape Fold Belt (Cape orogeny).

Illite crystallinity

In this study, the Kübler index (KI) was used as a rough geothermometer. The Kübler index is a type of illite crystallinity index (Eberl and Velde, 1989), which is the value given to the width of the 10Å (001) illite peak at half its maximum height in XRD reflection (Kübler, 1964, 1967). The values obtained during analysis of the (001) illite peak were calibrated to the crystallinity index standard (CIS) as proposed by Warr and Rice (1994).

The Kübler index values need to be interpreted with caution, because they only allow for the semi-quantitative determination of the degree of metamorphism in very low-grade pelitic rocks (Eberl and Velde, 1989; Fagereng and Cooper, 2010). In mudstones, the metastable clay minerals have a reaction sequence that comprises three stages: the diagenetic zone, the anchizone and the epizone, which have corresponding vitrinite reflectance values of

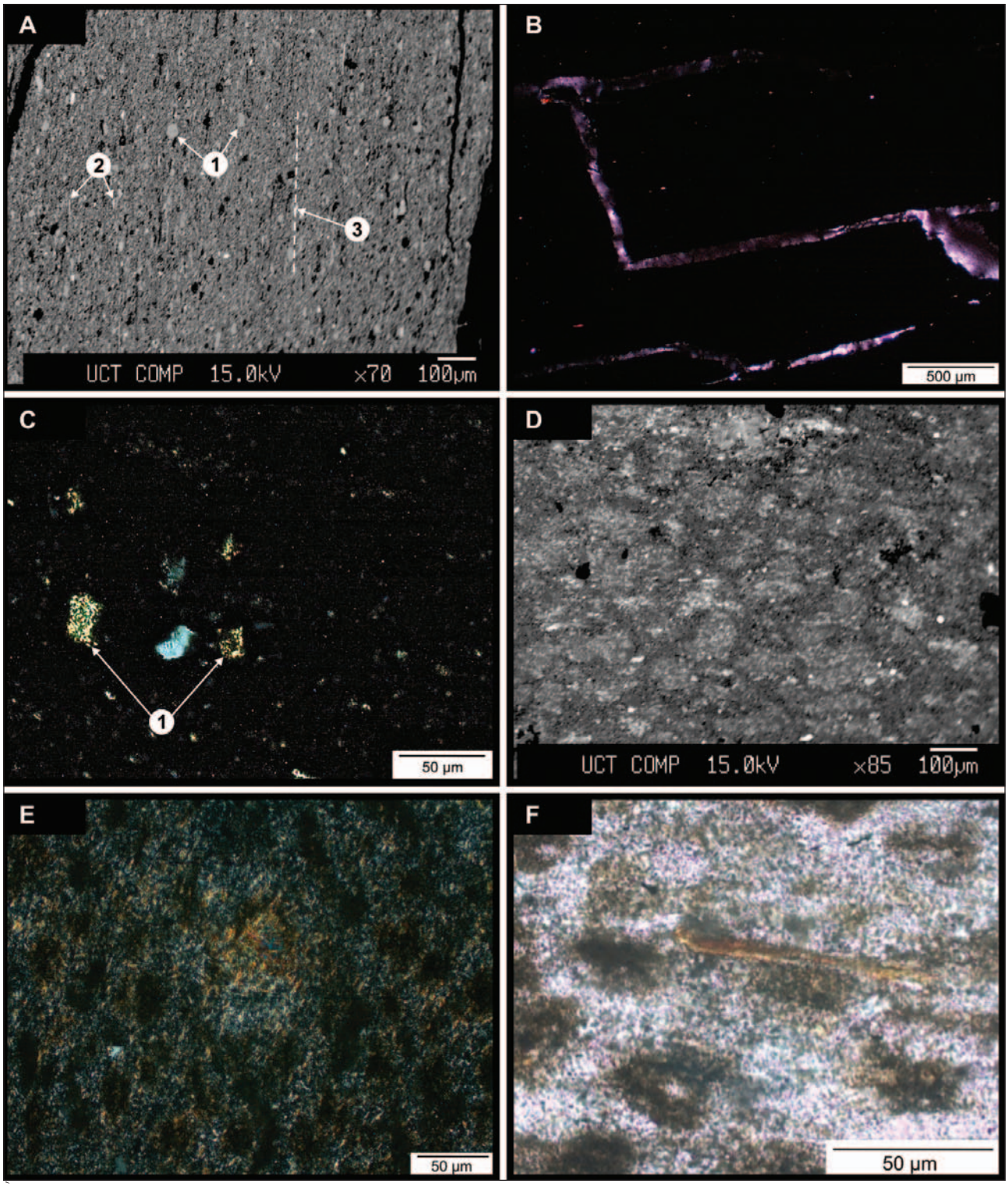

Figure 8. *Photomicrographs of the Whitehill Formation samples 16 (shown in A, B, C) and 17 (shown in D, E, F) taken 3 m and 3.3 m away from a dolerite sill, respectively (Calvinia area, Northern Cape, South Africa). (**A**) Sedimentary lamination indicated by lath-shaped detrital grains (e.g., albite: 1) and possible preferred orientation of authigenic muscovite (2) sub-parallel to lamination (dashed line for weak foliation?) (back-scattered electron image). (**B**) Fibrous quartz vein in sample 16 (in cross-polarised light). (**C**) Sericitisation (1) of pre-existing mineral grains (in cross-polarised light). (**D**) Incipient hornfels texture in sample 17 containing diffuse clots of quartz-albite-muscovite (1) and phengite-muscovite (2) assemblages (back-scattered electron image). (**E**) Radial growth of authigenic micas (in cross-polarised light). (**F**) Mica lath with straight extinction (in cross-polarised light. For location and other details of these samples, see Appendix 1.*

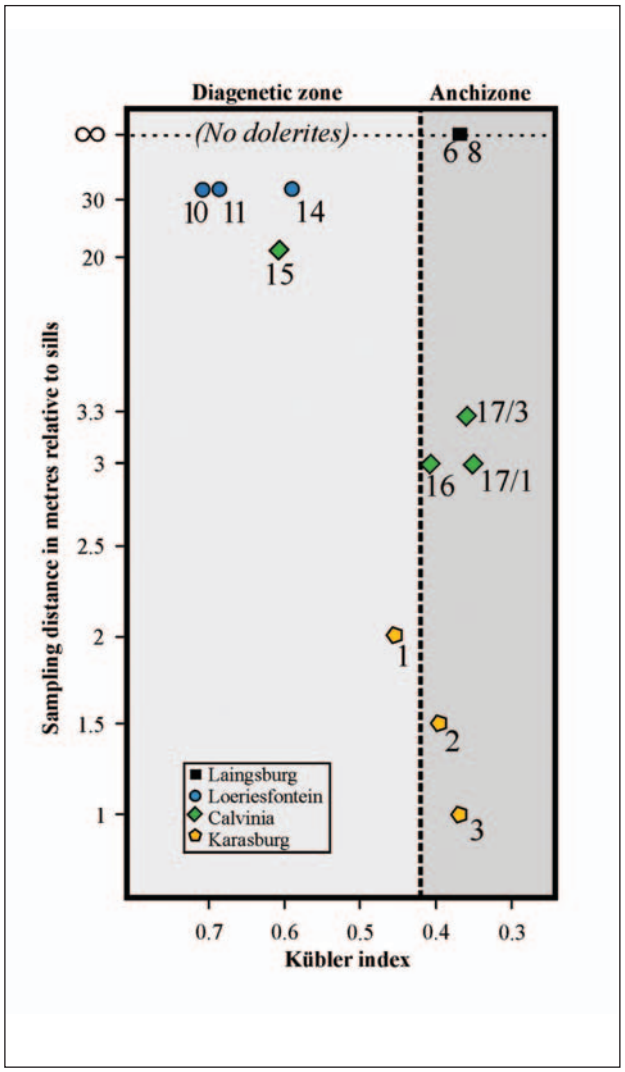

***Figure 9**. Plot of illite crystallinity (KI or Kübler index) versus the sampling distance relative to the dolerites. Sample 17 from Calvinia is made up of multiple chips over a distance of 1 m, hence the suffix /1 and /3. Metapelitic zone boundaries from Warr and Rice (1994). For location and other details of these samples, see Appendix 1.*

2.00%, 3.00% and 4.00%, respectively. Warr (1996) defined the anchizone as a transition between the diagenetic zone with a KI (001) >0.42 Δ°2Θ and the metamorphic epizone with a KI (001) <0.25 Δ°2Θ. Unlike vitrinite reflectance (Ro) values, which are the most commonly cited proxy for peak temperatures and organic maturation, the KI values are not absolute geothermometers providing quantitative information on the peak temperatures. The latter, however, has a negligible correlation with regard to geological time and thus its applicability is also inadequate in isolation. It has been shown that the temperature indicated by illite crystallinity data is often lower than that indicated by vitrinite reflectance due to the slow reaction rates of clay minerals relative to temperature-sensitive organic-matter (Teichmüller, 1987). More specifically, clay minerals do not reflect thermodynamic equilibria, because the intermediate compositions in diagenetic and low grade metamorphic conditions are highly dependent on reaction kinetics. Therefore, although mineral compositions cannot be linked to particular P-T conditions, they can be associated with an attained stage in the reaction sequence (Merriman and Peacor, 1999).

In this study the use of Kübler index rather than vitrinite reflectance is preferred as the ability of the source rock to produce tight-gas is not as much a function of organic matter maturity as it is the preservation of pore spaces in the source rock, primarily in its the organic matter (Milliken et al., 2013). Note that Rowsell and De Swart (1976) express Kübler Index as the width in millimetres of the 10Å diffraction peak at half its height, which is equivalent to 10 x Δ°2Θ value used in this study.

Samples from the localities intruded by dolerites (southern Namibia and Calvinia) are characterized by low KI values and thus plot in the anchizone of Warr and Rice (1994), suggesting significant recrystallization (Figure 9; Appendix 1). A higher KI value is observed the Calvinia sample 15, but its location furthest from the sill contact (20 m) makes it comparable with those from Loeriesfontein. Laingsburg also plots in the low KI anchizone and would indicate recrystallization, possibly due to the regional tectonic overprint (Cape orogeny). Sample 14 from Loeriesfontein has an anomalously low KI, perhaps reflecting a syn-sedimentary crystalline detritus or a secondary overprint.

A further evaluation of the significance of KI is displayed in Figure 10, where this estimate of illite crystallinity is compared with the ratio of the (002) and (001) XRD lines. While this ratio is primarily controlled by the Al/(Mg+Fe) ratio in the octahedral sites of the illite (Weaver, 1984, p. 81), it has been suggested the KI data are more diagnostic of thermal recrystallization in more Al-illites with (002)/(001) ratios >0.3 (Fisch, 1983). Most of the analysed samples satisfy this stipulation and thus confirm the relationship between KI and distance (Figure 9). The trend in increasing Al/(Mg+Fe) in illite with recrystallization and thus metamorphic grade has also been reported in the review by Weaver (1984, p. 82), and while some rudimentary trend curve could perhaps be drawn through the data in Figure 10, the significance of this is still open to question given to low number of samples. Two samples appear to deviate from the main grouping, to lower (002)/(001) ratios suggestive of higher Mg+Fe, and would thus be inconsistent with such a metamorphic control. The results suggest rather that illite crystallinity may not be controlled by chemical composition. Finally, the illite crystallinity results show a maximum temperature of ≤300°C, thereby indicating a relatively low degree of metamorphism, both in terms of contact phenomena (sill intrusion) and regional tectonic overprint (Cape orogeny).

Geochemistry

Variation in chemical composition of the Whitehill Formation has been assessed in terms of possible effects

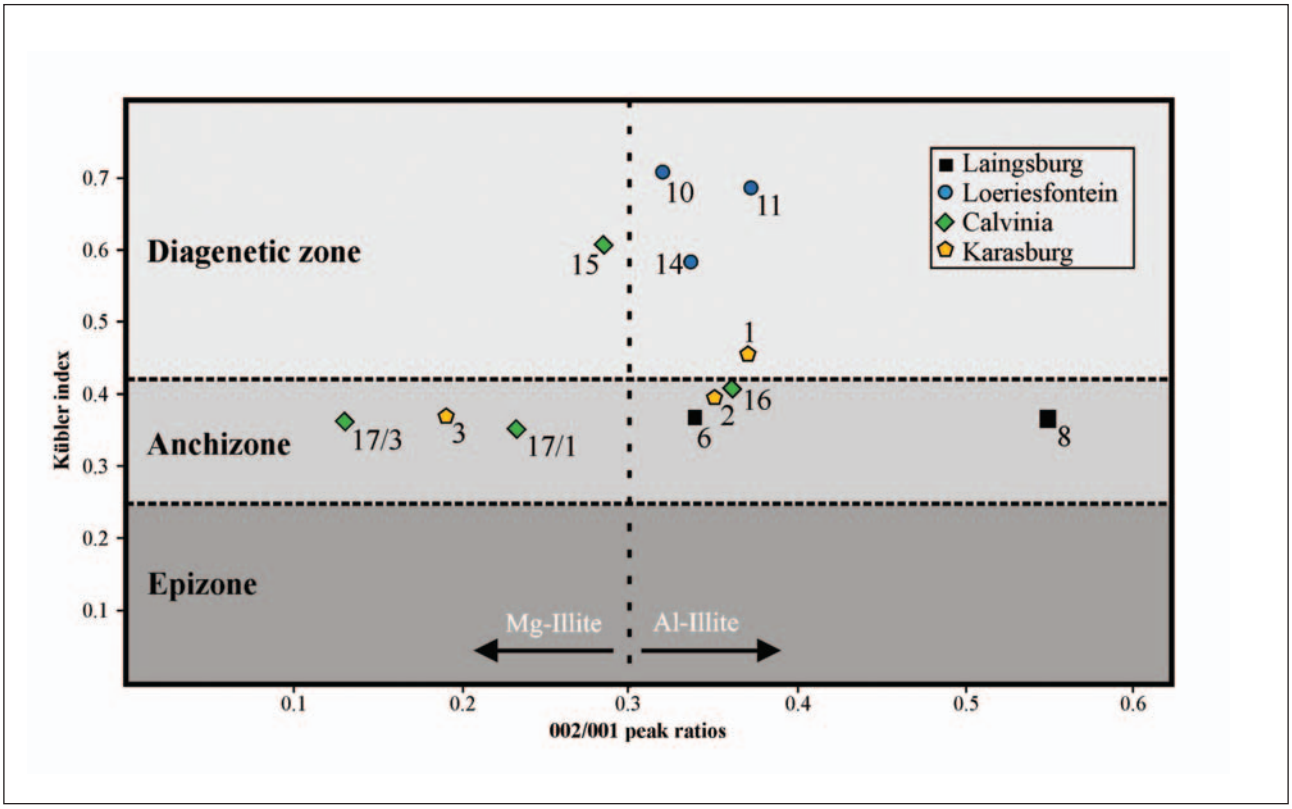

Figure 10. *Plot of illite crystallinity (KI or Kübler index) versus the ratio of (002) to (001) illite peaks, essentially a measure of the Al/(Mg+Fe) ratio in the octahedral site of the illite structure (Fisch, 1983). The (002)/(001) ratios are mainly >0.3, and thus support the thermal significance of KI (Fisch, 1983). Metapelitic zone boundaries from Warr and Rice (1994). For location and other details of these samples, see Appendix 1.*

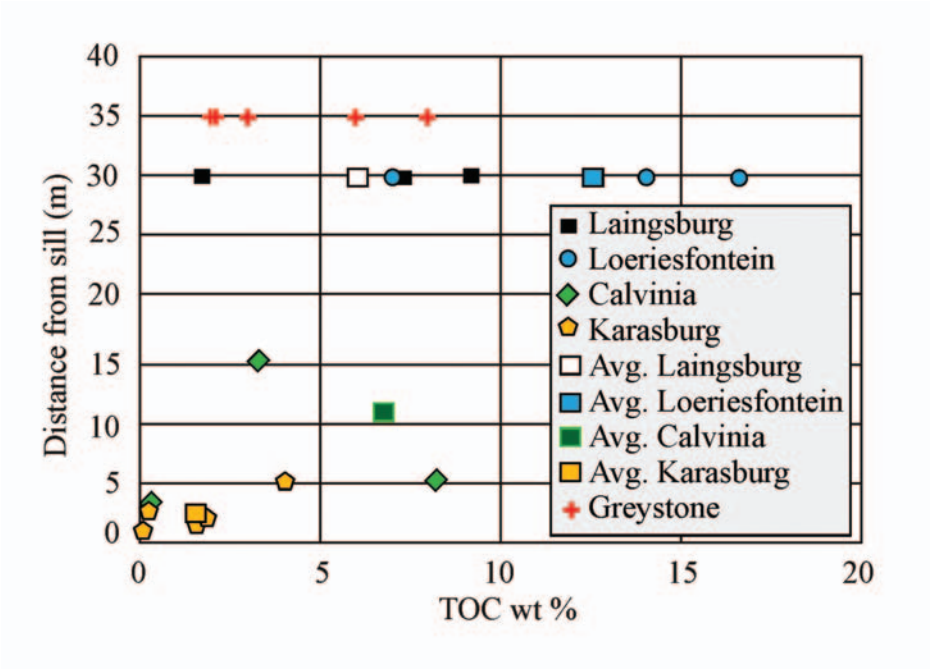

Figure 11. *Plot of Total Organic Carbon (TOC) in Whitehill Formation samples versus distance from the dolerite sill contact (in metres). Samples from areas unaffected by dolerites (Loeriesfontein and Laingsburg) have been placed arbitrarily at 30 m, while those from Greystone (Geel et al., 2013) are at 35 m for sake of clarity.*

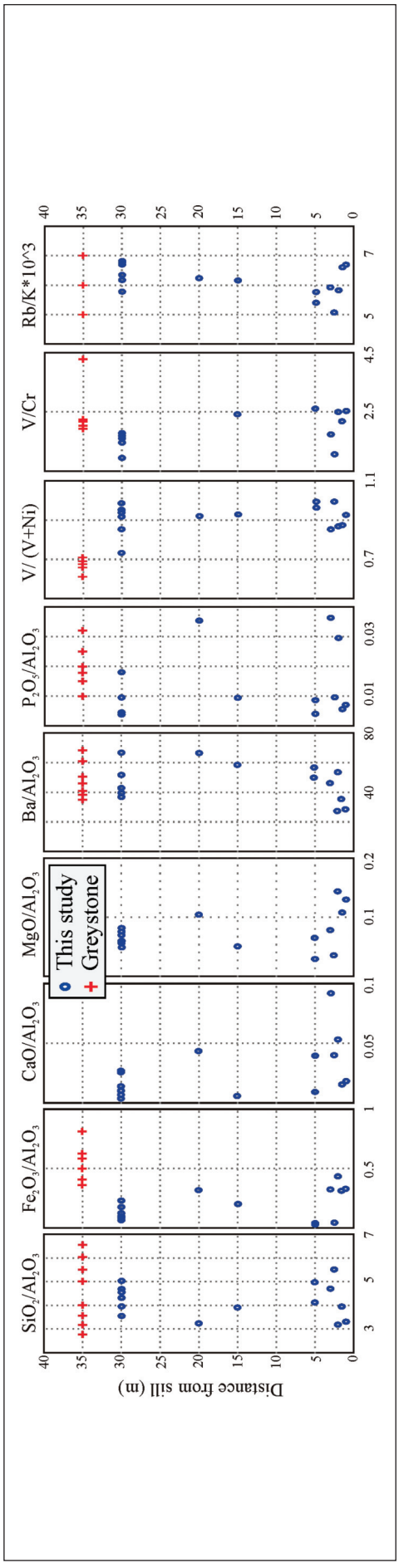

Figure 12. *Behaviour of major oxide and selected trace element ratios in Whitehill Formation samples. Traditionally used to characterise depositional conditions and provenance of sediments (cf. Geel et al., 2013), these ratios have been plotted against distance from the dolerite sill contact (in metres). Samples from areas unaffected by dolerites (Loeriesfontein and Laingsburg) have been placed arbitrarily at 30 m, while those from Greystone (Geel et al., 2013) are at 35 m for sake of clarity.*

from igneous intrusion using major and trace element data determined on whole rock powders by XRF (Appendix 1). The LOI (loss on ignition at 950°C) value is a combination of TOC (organic carbon) and H_2O+ (chemically bound water), since no significant carbonate was detected in any of the analysed samples; the latter was confirmed by the negligible CaO contents (<1%). In addition, the Fe content in all samples is very low (<5 weight %) and thus gain on ignition by oxidation of ferrous iron (e.g., due to modal pyrite) is negligible.

Reduction in volatile content is indicated by the plot of TOC versus distance from the sill contact (Figure 11), with the Karasburg Basin (southern Namibia) samples being the most affected (<2%). The Calvinia samples were further from sill contacts and show less depletion (average 5.2%). No sills are present at Loeriesfontein and while the variation in TOC is marked, on average the Whitehill Formation at this locality displays the highest levels of organic carbon (~6.3%). The Laingsburg locality is also free of intrusive sills but its more southerly position places it in the zone of the Cape Fold Belt (CFB), and its lower average TOC (3.6%) is probably a regional metamorphic effect, similar to that reported by Geel et al. (2013) in the Greystone area further east in the CFB (average 4.5%). Judging from the range in TOC observed at Loeriesfontein, which is probably the least affected area in terms of igneous intrusion and tectono-thermal effects, the original organic carbon content of the Whitehill Formation was at least 15 to 20% in that region.

Possible open system behaviour of major oxides (and some trace elements) in the thermal aureole is assessed in Figure 12, where selected element ratios (traditionally used to characterise sediment provenance and depositional conditions) are plotted against distance from the sill contact. The SiO_2/Al_2O_3 ratio is usually taken as a proxy for quartz/clay or quartz/mica in the original sediment, and has been shown to vary between 3 and 7 at Greystone, but this represents a 26 m interval through the entire Whitehill Formation. If the chemical variation is more subdued at the cm – m scale, the fact that this spread is almost reproduced within a 5 m section next to the dolerite sill contact would perhaps suggest small-scale remobilisation of SiO_2 in hydrothermal veinlets. Fe_2O_3/Al_2O_3 ratios appear slightly lower in the analysed samples, compared with the results from the Greystone area. Again the range displayed close to the sill contact is slightly wider than that observed in the distal samples, perhaps suggesting some open system behaviour of Fe. The behaviour of CaO and MgO relative to Al_2O_3 is normally taken to reflect modal carbonate and the very low ratios are consistent with its absence in the analysed samples. There is however a greater variation in the samples close to the sill contact, particularly to higher values, and would be consistent with small-scale development and migration of carbonate. Behaviour of P_2O_5 and Ba indicate limited modification within the thermal

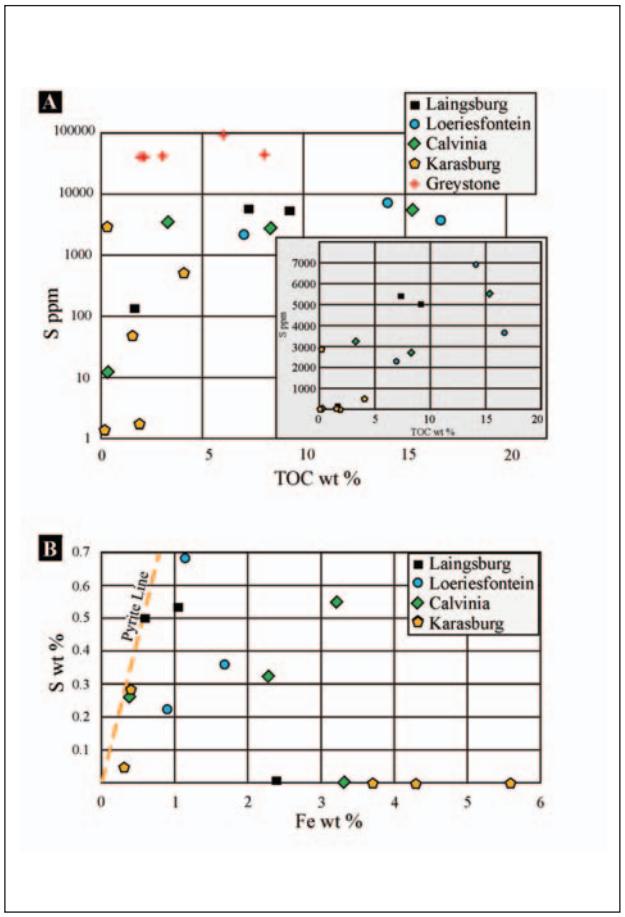

Figure 13. *(**A**) Plot of Total Organic Carbon (TOC) versus Sulfur (S) in the Whitehill Formation samples analysed in this study together with the higher S samples from Greystone (Geel et al., 2013) which necessitates a log scale in order to highlight the differences. Inset shows only the samples analysed in this study. (**B**) Plot of Fe versus S illustrating the departure of the samples analysed in this study from the pyrite control line (S:Fe = 1.15).*

aureole, a feature shared by the other provenance proxies V/(V+Ni), which is taken to reflect anoxic conditions (Rimmer, 2004), and Rb/K indicating marine salinity (Scheffler et al., 2006). In the case of V/Cr, two samples from Calvinia have extremely low values, due to the anomalously high Cr contents (>1000 ppm), but the remainder are uniformly higher and consistent with anoxia. To summarise, these geochemical proxies in the samples close to the sills do not show significant departures from those observed in samples remote from dolerite contacts.

The behaviour of sulphur in the Whitehill samples analysed in this study (Figure 13A) seems to depart from that observed at the Greystone locality by Geel et al. (2013). Firstly, the overall abundances are an order of magnitude lower (Figure 13A), with a range between near zero and only 0.7%, compared with 4 to 9% at Greystone. Secondly, there is a positive correlation between S and TOC (Figure 13B), which is not obvious in the Greystone data. The difference is further illustrated in the Fe-TOC-S plot in Figure 14, where all the Whitehill data are compared. At Greystone, Geel et al. (2013) interpret the compositional pattern as one of pyrite control, where the majority of samples preserve the limiting control of available Fe. In contrast, the S-depleted nature of the samples analysed in the present study is clearly shown by their compositions plotting very close to the Fe – TOC border. Only one sample has a relative S content sufficiently high so as to plot in the same field as Greystone, and those that plot near the TOC apex are ambiguous in the sense they could conceivably follow the pyrite control line but would demand extremely low primary Fe contents. Finally, those samples with relatively high Fe and plotting along the near zero S baseline are difficult to explain in terms of primary compositions, since they require an original sediment devoid of any marine sulphate-bearing pore water (Dean and McArthur, 1989). Rather they could be some product of S-depletion associated with thermal metamorphism, since all but one occur within 3 m of the sill contact.

Discussion

The variations in metamorphic mineral assemblages are routinely used to define subsurface P-T conditions through the geological evolution of pelitic rocks (Frey, 1987; Yardley, 1989). Notwithstanding the limited samples and results of this pilot study, the palaeo-temperature range for the Whitehill Formation, based on the Kübler index (KI) values can be constrained further by the mineral assemblages present in the Whitehill

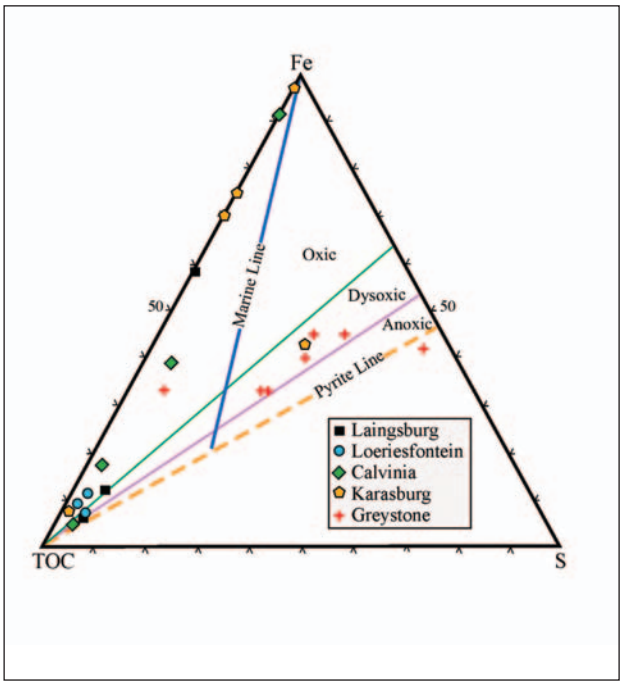

Figure 14. *Plot of Fe – TOC – S after Dean and McArthur (1989), showing the compositions of the samples analysed in the current study, together with the results from the Greystone area (Geel et al., 2013). Pyrite Line = all Fe in sample occurs in pyrite. Marine Line = average TOC/S ratio in young marine organic-rich shales.*

Formation that are close to the dolerites (Figures 5 to 10; Appendix 1). Dehydration reactions are primarily dependant on the rate of heat input into the system, and therefore assuming a contact aureole temperature of ~500°C, the reaction, leading to incipient recrystallisation of the sedimentary fabric, could be completed in ~200 years (Walther and Wood, 1984). Minerals such as chlorite and phengitic muscovite as well as the lack of authigenic biotite are indicative of a maximum subsurface temperature of ≤300°C, i.e. chlorite zone conditions (Yardley, 1989). These chlorite zone (lower greenschist facies) mineral assemblages in our samples (Figures 5 and 7; Tables 1 and 2) are significant in constraining the contact metamorphic aureole thickness. The limited duration of heating, however, could have inhibited the formation of potentially higher-grade minerals. Nevertheless, based on the average across the samples with recrystallisation features, the maximum temperature of ≤300°C necessary for the formation of very-low grade minerals, is indicative of the localised long-term effective temperature induced by the dolerite intrusions. This is observed by the distinction between samples 16 and 17, collected close to the dolerite in Calvinia as well as the samples 10 and 11 taken 60 km north of Calvinia, at Loeriesfontein a sampling locality free of outcropping dolerites (Figures 9, 10). Assuming that burial metamorphism has a regional effect, similar metamorphic signatures would be expected at these nearby localities in the northwestern Karoo Basin, yet the Loeriesfontein samples show a much lower degree of metamorphism (i.e., diagenetic zone).

During burial diagenesis of pelitic sediments, the transformation of clay minerals is primarily affected by temperature; hence this is the key physical factor affecting illite crystallinity (Kübler, 1964, 1967; Warr, 1996; rodo , 1999; Fagereng and Cooper, 2010). It is most likely that the entire Whitehill Formation experienced burial diagenesis prior to any subsequent thermal perturbations brought about by orogenic (i.e., Cape Fold Belt) or igneous (i.e., Karoo dolerites) events. Loeriesfontein is the most northerly situated locality of the main Karoo Basin and thus is the least likely to have experienced effects of the southern Cape Fold Belt. Furthermore, tectonism responsible for the syntaxis and the north-striking folds that occur in the Western Cape from Ceres to Clanwilliam does not appear to extend to Calvinia, let alone Loeriesfontein. However this latter locality is situated on the western edge of the Karoo dolerite province (Svensen et al., 2015) and contact thermal effects may be anticipated. The highest TOC-bearing Whitehill Formation samples at Loeriesfontein also display the highest KI and thus represent to closest approach to a pre-metamorphic (= burial diagenetic) signature, considered to be <180°C or the base of the "oil-window" (cf. Quigley and MacKenzie, 1988). Elevated inferred temperatures produced by contact thermal metamorphism are recorded at Calvinia and in the Karasburg Basin (southern Namibia), having the lowest KI and TOC values, which correspond to a temperature below the anchizone-epizone transition, generally accepted to be <300°C (Merriman and Peacor, 1999). Inferred temperatures at Laingsburg are interpreted to be the product of orogenic regional metamorphism under sub-greenschist facies conditions (~280°C).

These results signify a decrease in the degree of thermal pertubation, from sub-greenschist alteration in the south to burial diagenetic conditions in the north, within the main Karoo Basin, which correlates well with previously published results (Rowsell and de Swardt, 1976; Cole and McLachlan, 1991; Frimmel et al., 2001). Earlier regional studies (e.g., Rowsell and de Swardt, 1976) sampled and averaged various Karoo mudstones in a range of burial depths and did not sample the far northwestern main Karoo Basin, hence the high KI values of Loeriesfontein samples cannot be related to the regional trends. The marked variation in the illite crystallinity values samples from near Calvinia (Figures 9, 10) could be explained by the potential insulation and increased temperature generated by the two parallel dolerites that allowed for a greater period of heating, and therefore recrystallization of illite in samples 17-1 and 17-3 relative to sample 16.

Our investigation of geochemical patterns in proximity to dolerite sills has not produced results indicative of significant open system behaviour (Figures 11 to 14). Most of the compositional variation observed in +/- 5 m contact profiles can equally be explained by facies changes inherent in the sedimentary record, subject to provenance and depositional conditions.

Volatile components such as TOC and H_2O^+ do however appear to be reduced in the thermal metamorphic aureole, as witnessed in southern Namibia and Calvinia, but also as a consequence of regional metamorphism in the Cape Fold Belt, such as at Laingsburg and Greystone. Primary TOC levels in the Whitehill Formation are therefore inferred to have been significantly higher than the average ~4.5% commonly cited for the unit (see Geological Background), but may only be preserved very locally in areas unaffected by dolerite intrusion or orogeny, such as Loeriesfontein. Even at this latter locality, the distribution of dolerite sills is highly irregular, with heavily intruded strata occurring a few km away. Orogenically induced devolatization is likely to be quite pervasive, but our study indicates the possible preservation of high TOC zones within the Whitehill Formation throughout the Karoo dolerite province. Strata that are >30 m away from dolerite contacts may represent a useful guide in this context.

Another interesting geochemical result of the present study is the seemingly very depleted sulphur contents. In contrast to the Greystone area studied by Geel et al. (2013), our study localities have less than 1% sulphur content and are difficult to explain. If it is a primary feature, then it represents some syn-depositional process

that restricted the amount of sulphate in the pore waters, perhaps indicative of a non-marine environment. This is not consistent with the salinity proxy, the Rb/K ratio. There is a rough positive correlation between TOC and total sulphur, but comparison with Greystone data indicates an order of magnitude lower sulphur for a given TOC. Alternatively the low sulphur may have been caused by a secondary effect, where original diagenetic pyrite (or organically hosted S) was altered and/or weathered to allow the release of oxidised sulphur. Abundant field evidence for the mobility of S in the surface outcrops (yellow effluorescence, white gypsum effluorescence, fetid odours) would be consistent with this. Should this low S feature be an inherent property of the Whitehill Formation, and not a result of surface weathering (e.g., the Greystone study was based on drill core), then maybe these alternative localities could be considered a low sulphur hydrocarbon resource.

Hydrocarbon potential

To date, geological consensus (e.g., Rowsell and de Swardt, 1976; Anderson and McLachlan, 1979) holds that the Whitehill Formation has undergone at least strong burial diagenetic metamorphism, and therefore it is within the "over-mature" metagenesis stage with respect to hydrocarbon generation. Tight-gas production relies on the ability of the source rocks to retain some of the produced hydrocarbon in pore spaces within the rock, most of all in its organic matter (Milliken et al., 2013). In the case of pelites, the conversion of organic matter into graphite, as well as the metamorphic micro-recrystallisation and subsequent destruction of pore spaces, are two potential inhibitors to the preservation of reservoir quality methane within the Whitehill Formation (Laughrey et al., 2011). Graphitisation commonly occurs in metapelitic rocks as a result of regional or contact metamorphism at a temperature range of 350 to 600°C and at pressures of ~0.4 GPa (Teichmüller, 1987; Luque et al., 1998). Similarly, Stoll and Nover (2001) reported the generation of graphite within a shear stressed environment at 354 to 514°C and 100 to 170 MPa, respectively. Therefore, the conversion of organic matter to graphite, and concurrent loss of light hydrocarbons, is reported to take place at temperatures >350°C and pressures >100 MPa (Stoll and Nover, 2001).

More recently, Maré et al. (2014), using magnetic fabric as a geothermometric proxy, showed that the re-magnetization of the Karoo host rocks does not exceed distances more than half the sill thicknesses, and thus suggest that preservation of hydrocarbons between the widely spaced Karoo intrusions is possible in the western main Karoo Basin. Considering that Svensen et al. (2015) document that most sills (~80%) in the Ecca Group are less than 30 m thick and are widely spaced (>100 m) in the western main Karoo Basin, where the observed thickness of the Whitehill Formation is ~70 m, a reasonable preservation potential for hydrocarbons within the shales of the Formation may be expected. However, these expectations need to be balanced against the following: (1) the dolerite sills appear to have preferentially intruded the Whitehill Formation (D. Cole, personal communication), and (2) the Whitehill reservoir has been possibly depressurised due to its shallow subsurface position in the westernmost Karoo Basin (J. Decker personal communication). Consequently, for the delineation of potential shale-gas preservation zones in the Lower Permian Whitehill Formation and for the characterization of the geological parameters of the overlying Karoo rocks, the systematic quantification of the effect of Jurassic Karoo dolerite intrusions on the host rocks in outcrops and cores is essential on a regional scale. Furthermore, there is a great need for the assessment of the subsurface 3-D geometries of the Karoo dolerite complex not only via integrated geophysical surveys (e.g., Scheiber-Enslin et al., 2014), but also though quantitative surface imaging and basic geological mapping methods (e.g., determining the spacing, thickness and attitude of the dolerites in outcrops by integrating photogeologic imaging, GIS and traditional field work).

Conclusion

In this pilot study, petrographic and geochemical data are used to estimate the geothermal effect of Jurassic Karoo dolerite intrusions on the hydrocarbon potential of the Permian Whitehill Formation in western South Africa and southern Namibia. We confirm that the Whitehill Formation in the southern main Karoo Basin has undergone very low grade metamorphism, i.e. lower anchizone, as a result of deep burial diagenesis and thermal effect of the Cape orogeny, as indicated by illite crystallinity values of 0.37 $\Delta°2\Theta$. The degree of burial diagenesis decreases further north as substantiated by KI(001) values >0.5 $\Delta°2\Theta$ north of 31°S. However, dolerite intrusions have in some places metamorphosed the Whitehill Formation shales to very low grades, validated by illite crystallinity values of ~0.35 $\Delta°2\Theta$. Additionally, the effect of multiple dolerite intrusions has been seen to greatly enhance the degree of local metamorphism suggested by the crystalline textures developed within the Whitehill Formation shales. Chlorite zone mineral assemblages, generally regarded to occur at temperatures ≤300°C, concur with the very low grade metamorphism suggested by the illite crystallinity values (Kübler, 1964; Frey, 1987; Yardley 1989; Cole and McLachlan, 1991).

In summary, the results from the assessment of the illite crystallinity, geochemical signatures and mineral assemblages of selected Whitehill Formation samples in this pilot study suggest that potential hydrocarbon preservation within the Formation might be possible beyond the contact aureole of the dolerite sills. Finally, this pilot study also highlights the acute need not only for the systematic quantification of the effect of Jurassic Karoo dolerites in outcrops and cores, but also for the assessment of the subsurface thickness and spacing of the Karoo intrusive bodies, via integrated quantitative

surface imaging, field work and subsurface geophysical surveys, thereby assisting with delineation of potential shale-gas preservation zones in the Lower Permian Whitehill Formation.

Acknowledgments

We thank the following of our colleagues at the Department of Geological Sciences (University of Cape Town): Francisco Paiva, Chelsea Rebelo and Adrian Bunge for their field assistance; Christel Tinguely, Tanya Dreyer, Dr Ake Fagereng and Dr John Compton for analytical assistance as well as David Wilson, Ernest Stout and Jonathan Van Rooyen for sample preparation assistance. Research funds received from the Harry Crossley Scholarship (by TS), Inkaba ye Afrika (by DR), National Research Foundation of South Africa (Incentive Funding for EB) and University of Cape Town (new staff start-up grant for EB) are gratefully acknowledged. The funding sources had no other involvement in this research. We are also very grateful to the Editor Jay Barton as well as to Michel de Kock, John Decker and an anonymous reviewer for improving this manuscript greatly through their comprehensive and constructive reviews. This is Inkaba Publication number 125.

References

Anderson, A, M. and McLachan, I.R., 1979. The Oil-Shale Potential of the White Band Formation in Southern Africa. Geological Society of South Africa Special Publication, 8, 83-89.

Byrnes, G., 2013. Flexural-slip folding mechanism in the Prince Albert Formation, Laingsburg. Unpublished BSc Honours Thesis, University of Cape Town, South Africa. 40pp.

Bangert, B., Stollhofen, H., Lorenz, V. and Armstrong, R., 1999. The geochronology and significance of ash-fall tuffs in the glaciogenic Carboniferous-Permian Dwyka Group of Namibia and South Africa. Journal of African Earth Sciences, 29, 33-49.

Bussio, J.P., 2012. Effect of dolerite intrusions on coal quality in the Secunda coal fields of South Africa. Unpublished MSc dissertation, University of Pretoria, South Africa, 90pp.

Catuneanu, O., Hancox, P.J. and Rubidge, B.S., 1998. Reciprocal flexural behaviour and contrasting stratigraphies: a new basin development model for the Karoo retroarc foreland system, South Africa. Basin Research, 10, 41-439.

Chevallier, L. and Woodford, A., 1999. Morpho-tectonics and mechanism of emplacement of the dolerite rings and sills of the Western Karoo, South Africa. South African Journal Geology, 102, 43-54.

Chevallier, L., Goedhart, M. and Woodford, A.C., 2001. The influence of dolerite sill and ring complexes on the occurrence of groundwater in Karoo Fractured Aquifers: a morpho-tectonic approach. WRC Report No. 937/1/01. 146pp.

Cole, D.I and Basson, W.A., 1991. Whitehill Formation. South African Committee for Stratigraphy, Catalogue of South African Lithostratigraphic Units, 51-52.

Cole, D.I. and McLachlan, I.R., 1991. Oil potential of the Permian Whitehill Shale Formation in the main Karoo Basin, South Africa. In: H. Ulbrich, and A.C. Rocha Campos (Editors), Gondwana Seven Proceedings, 379-390.

Cole, D.I., 1992. Evolution and development of the Karoo Basin. In: M.J. de Wit and I.G.D Ransome (Editors), Inversion tectonics of the Cape Fold Belt, Karoo and Cretaceous basins of Southern Africa, Balkema, Rotterdam, The Netherlands, 87-99.

Dean, W.E. and McArthur, M.A., 1989. Iron-sulfur-carbon relationships in organic-carbon-rich sequences: Cretaceous western seaway. American Journal of Science, 289, 708-743.

De Wit, M.J., 2011. The great shale debate in the Karoo. South African Journal of Science, 107, 1-9.

Dow, W.G., 1977. Kerogen studies and geological interpretations. Journal of Geochemical Exploration, 7, 79-99.

Duncan, R.A., Hooper, P.R., Rehacek, J., Marsh, J.S. and Duncan A.R., 1997. The timing and duration of the Karoo igneous event, southern Gondwana. Journal of Geophysical Research, 102, 127-138.

Eberl, D.D. and Velde, B., 1989. Beyond the Kübler Index. Clay Minerals, 24, 571-577.

Fagereng, Å. and Cooper, A. F., 2010. The metamorphic history of rocks buried, accreted and exhumed in an accretionary prism: an example from the Otago Schist, New Zealand. Journal of Metamorphic Geology, 28, 935-954.

Faure, K. and Cole, D., 1999. Geochemical evidence for lacustrine microbial blooms in the vast Permian Main Karoo, Parana, Falkland Islands and Huab basins of southwestern Gondwana. Palaeogeography, Palaeoclimatology, Palaeoecology, 152, 189-213.

Fildani, A., Drinkwater, N.J., Weislogel, A., McHargue, T., Hodgson, D.M. and Flint, S.S., 2007. Age controls on the Tanqua and Laingsburg deep-water systems: New insights on the evolution and sedimentary fill of the Karoo Basin, South Africa. Journal of Sedimentary Research, 77, 901-908.

Fisch, H.J., 1983. Mineralogy and petrology of burial diagenesis (burial metamorphism) and incipient metamorphism in clastic rocks. In: Larsen, G., Chilingar, G.V. (Editors), Diagenesis in sediments and sedimentary rocks 2. Elsevier Amsterdam, 289-494.

Frey, M., 1987. Very low-grade metamorphism of clastic sedimentary rocks. In: M. Frey (Editor), Low Temperature Metamorphism. Blackie, Glasgow, U.K., 9-57.

Frimmel, H.E., Fölling, P.G. and Diamond, R., 2001. Metamorphism of the Permo-Triassic Cape Fold Belt and its basement, South Africa. Mineralogy and Petrology, 73, 325-346.

Galushkin, Y. I., 1997. Thermal effects of igneous intrusions on maturity of organic matter: a possible mechanism of intrusion. Organic Geochemistry, 26, 645-658.

Geel, C., Schulz, H-M., Booth, P., De Wit, M. and Horsfield, B., 2013. Shale gas characteristics of Permian black shales in South Africa: results from recent drilling in the Ecca Group Eastern Cape. Energy Procedia, 40, 256-265.

Golab, A.N. and Carr, P. F., 2004. Changes in geochemistry and mineralogy of thermally and geochemically altered coal, Upper Hunter Valley, Australia. International Journal of Coal Geology, 57, 197-210.

Hargraves, R.B., Rehacek, J. and Hooper, P.R., 1997. Palaeomagnetism of the Karoo igneous rocks in southern Africa. South African Journal Geology, 100, 195-212.

Johnson, M.R., 1976. Stratigraphy and sedimentology of the Cape and Karoo sequences in the Eastern Cape Province. Unpublished PhD Thesis, Rhodes University, South Africa. 366pp.

Johnson, M.R., Van Vauuren, C.J., Hegenberger, W.F., Key, R. and Shoko, U., 1996. Stratigraphy of the Karoo Supergroup in southern Africa: an overview. Journal of African Earth Sciences, 23, 3-15.

Johnson, M.R., Van Vuuren, C.J., Visser, J.N.J., Cole, D.I., Wickens, H. De V., Christie, A.D.M. and Roberts, D.L., 1997. The Foreland Karoo Basin. In: R.C Selley (Editor), African Basins. Sedimentary Basins of the World, 3, 269-317.

Kingsley, C.S., 1985. Stratigraphy and sedimentology of the Ecca Group in the Eastern Cape Province. Unpublished PhD Thesis, University of Port Elizabeth, South Africa. 286pp.

Krynauw, J.R., Hunter, D.R. and Wilson, A.H., 1994. Sill emplacement in wet sediments: fluid inclusion and cathodoluminiscenece studies at Grunehogna, western Dronning Maud Land, Antartica. Journal of the Geological Society, London, 151, 777-794.

Kübler, B., 1964. Les argiles indicateurs de métamorphisme. Revue Instituté de la Français de Pétrole, 19, 1093-1112.

Kübler, B., 1967. La cristallinité de l'illite et les zones tout à fait supérieures du métamorphisme. In: Étages tectoniques, Colloque de Neuchâtel, 1966, À la Baconnière, Neuchâtel, Suisse, 105-121.

Laughrey, C.D., Ruble, T.E., Lemmens, H., Kostelnik, J., Butcher, A.R., Walker, G. and Knowles, W., 2011. Black shale diagenesis: Insights from integrated high-definition analyses of postmature Marcellus Formation rocks, northeastern Pennsylvania. AAPG Search and Discovery Article #90122©2011 AAPG Hedberg Conference, December 5-10, 2010, Austin, Texas, U.S.A.

López-Gamundí, O.R., Conaghan, P.J., Rossello, E.A. and Cobbold, P.R., 1995. The Tunas Formation (Permian) in the Sierras Australes Foldbelt, east central Argentina: evidence for syntectonic sedimentation in a foreland basin. Journal of South American Earth Sciences, 8, 129-142.

Luque, F.J., Pasteris, J.D., Wopenka, B., Rodas, M. and Barrenechea, J.F., 1998. Natural Fluid Deposited Graphite: Mineralogical Characteristics and Mechanisms of Formation. American Journal of Science, 298, 471-498.

Maré, L.P., de Kock, M.O., Cairncross, B. and Mouri, H., 2014. Application of magnetic geothermometers in sedimentary basins: an example from the western Karoo Basin, South Africa. South African Journal of Geology, 117, 1-14.

Marsh, J.S., Hooper, P.R., Rehacek, J., Duncan, A.R. and Duncan, R.A., 1997. Stratigraphy and age of Karoo basalts of Lesotho and implications for correlations within the Karoo Igneous Province. In: J.J. Mahoney and M. Coffin (Editors), Large Igneous Provinces. Geophysical Monograph, 100, 247-272.

Quigley, T.M. and MacKenzie, A.S. 1988. The temperature of oil and gas formation in the subsurface. Nature, 33, 549-552.

Merriman, R.J. and Peacor, D.R., 1999. Very low-grade metapelites: mineralogy, microfabrics and measuring reaction progress. In: M. Frey and D. Robinson (Editors), Low-Grade Metamorphism. Blackwell Science, Oxford, UK, 10-60.

Milliken, K.L., Rudnicki, M., Awwiller, D.N. and Zhang, T., 2013. Organic matter-hosted pore system, Marcellus Formation (Devonian), Pennsylvania. AAPG Bulletin, 97, 177-200.

Oelofsen, B.W., 1981. An anatomical and systematic study of the Family Mesosauridae (Reptilia: Proganosauria) with special reference to its associated fauna and palaeoecological environment in the Whitehill Sea. Unpublished PhD thesis, University of Stellenbosch, South Africa. 259pp.

Oelofsen, B.W., 1987. The biostratigraphy and fossils of the Whitehill and Iratí Shale Formations of the Karoo and Paraná Basins. In: C.D. McKenzie (Editor), Gondwana Six: stratigraphy, sedimentology and paleontology. Geophysical Monograph, 41, 131-138.

Oelofsen, B.W. and Araújo, D.C., 1983. Palaeoecological implications of the distribution of mesosaurid reptiles in the Permian Irati Sea (Paraná Basin), South America. Revista Brasileira de Geociências, 13, 1-6.

Price, L., 1995. Origins, characteristics, controls, and economic viabilities of deep-basin gas resources. Chemical Geology, 126, 335-349.

Raymond, A.C. and Murchison, D.G., 1988. Development of organic maturation in the thermal aureoles of sills and its relation to sediment compaction. Fuel, 67, 1599-1608.

Rimmer, S.M., 2004. Geochemical paleoredox indicators in Devonian-Mississippian black shales, Central Appalachian Basin (USA). Journal of Chemical Geology, 206, 373-391.

Rowsell, D.M. and de Swardt, A.M.J., 1976. Diagenesis in Cape and Karroo sediments, South Africa, and its bearing on their hydrocarbon potential. Transactions of the Geological Society of South Africa, 79, 81-145.

Rubidge, B.S., Hancox, P.J. and Catuneanu, O., 2000. Sequence analysis of the Ecca-Beaufort contact in the southern Karoo of South Africa. South African Journal Geology, 103, 81-96.

Rubidge, B.S., 2005. Re-uniting lost continents -Fossil reptiles from the ancient Karoo and their wanderlust. South African Journal Geology, 108, 135-172.

Scheffler, K., Buehmann, D. and Schwark, L., 2006. Analysis of late Palaeozoic glacial to postglacial sedimentary successions in South Africa by geochemical proxies – Response to climate evolution and sedimentary environment. Palaeogeography, Palaeoclimatology, Palaeoecology, 240, 184-203.

Scheiber-Enslin, S., Webb, S.J. and Ebbing, J., 2014. Geophysically Plumbing the Karoo. South African Journal of Geology, 117, 275-300. doi:10.2113/gssajg.117.2.275.

Senger, K., Buckley, S.J., Chevallier, L., Fagereng, Å., Galland, O., Kurz, T.H., Ogata, K., Planke, S. and Tveranger, J., 2015. Fracturing of doleritic intrusions and associated contact zones: Implications for fluid flow in volcanic basins. Journal of African Earth Sciences, 102, 70-85. doi:10.1016/j.jafrearsci.2014.10.019

Środoń, J., 1999. Nature of mixed-layer clays and mechanism of their formation and alteration. Annual Reviews of Earth and Planetary Science, 27, 19-53.

Stoll, J. and Nover, G., 2001. Graphitisation of carbon-a P,T-laboratory experiment. In: A. Hördt and J. Stoll. (Editors), Protocoll zum 19. Kolloquim "Elektromagnetische Teifenforschung", Deutshce Geophysikalische Gesellschaft DGG, 1-7.

Stollhofen, H., Stanistreet, I.G., Bangert, B. and Grill, H., 2000. Tuffs, tectonism and glacially related sea-level changes, Carboniferous-Permian southern Namibia. Palaeogeography, Palaeoclimatology, Palaeoecology, 161, 127-150.

Svensen, H., Corfu, F, Polteau, S., Hammer O. and Planke, S., 2012. Rapid magma emplacement in the Karoo Large Igneous Province. Earth and Planetary Science Letters, 325-326, 1-9.

Svensen, H., Polteau, S., Caweighthorn, G. and Planke, S., 2015. Sub-volcanic intrusions in the Karoo Basin, South Africa. In: C. Breitkreuz and S. Rocchi, (Editors), Physical Geology of Shallow Magmatic Systems: Advances in Volcanology, Chapter 11, Springer. ISBN 978-3-319-14083-4 doi: 10.1007/11157_2014_7

Tankard, A., Welsink, H., Aukes, P., Neweighton, R. and Stettler E., 2012. Geodynamic interpretation of the Cape and Karoo basins, South Africa. In: Roberts, D.G., Bally, A.W. (Editors), Regional Geology and Tectonics: Phanerozoic Passive Margins, Cratonic Basins and Global Tectonic Maps. Elsevier, U.K., 869-945.

Teichmüller, M., 1987. Organic material and very low-grade metamorphism. In: M. Frey (Editor), Low Temperature Metamorphism. Glasgow, Blackie, 114-161.

Visser, J.N.J. and Loock, J.C., 1978. Water depth in the Main Karoo Basin, South Africa, during Ecca (Permian) sedimentation. Transactions of the Geological Society of South Africa, 81, 185-191.

Visser, J.N.J., 1992. Deposition of the Early to Late Permian Whitehill Formation during a sea-level highstand in a juvenile foreland basin. South African Journal Geology, 95, 181-193.

Visser, J.N.J., 1993. Sea-level changes in a back-arc-foreland transition: the Late Carboniferous-Permian Karoo Basin of South Africa. Sedimentary Geology, 83, 115-131.

Walther, J.V. and Wood, B.J., 1984. Rate and mechanism in prograde metamorphism. Contributions to Mineralogy and Petrology, 88, 246-259.

Wang, D., 2012. Comparable study on the effect of errors and uncertainties of heat transfer models on quantitative evaluation of thermal alteration in contact metamorphic aureoles: Thermophysical parameters, intrusion mechanism, pore-water volatilization and mathematical equations. International Journal of Coal Geology, 95, 12-19.

Warr, L.N., 1996. Standardised clay mineral crystallinity data from very-low grade metamorphic facies rocks of southern New Zealand, European Journal of Mineralogy, 8, 115-127.

Warr, L.N. and Rice, N., 1994. Interlaboratory standardization and calibration of clay mineral crystallinity and crystallite size data. Journal of Metamorphic Geology, 12, 141-152.

Weaver, C.E., 1984. Shale-Slate metamorphism in the southern Apalachians. Springer Amsterdam. 237pp.

Werner, M., 2006. The stratigraphy, sedimentology and age of the Late Palaeozoic Mesosaurus Inland Sea, SW-Gondwana: new implications from studies on sediments and altered pyroclastic layers of the Dwyka and Ecca Group (lower Karoo Supergroup) in southern Namibia. Unpublished PhD Thesis, University of Würzburg, Germany. 428pp.

Yardley, B.W.D., 1989. An introduction to Metamorphic Petrology. Harlow: Longman; New York: John Wiley and Sons Inc., 60-85.

Zagorski, W.A., Wrightstone, G.R. and Bowman, D.C., 2012. The Appalachian Basin Marcellus gas play: Its history of development, geologic controls on production and future potential as a world-class reservoir. In: J.A. Breyer (Editor), Shale reservoirs – Giant resources for the 21st century. AAPG Memoir 97, 172-200.

Editorial handling: J.M. Barton Jr.

Appendix table 1.

Sample		Locality	Position relative to sill	GPS Co-ordinates	Mineralogy	XRF	XRD	Kubler index Illite crystallinity (Δ°2:Θ)	Sample
1	TS-1	Karasburg (Nam)	2 m below	28°34'06.5"S 17°39'21.0"E	not analyzed	see Sheet 2	not analyzed	0.46	1
2	TS-2	Karasburg (Nam)	1.5 m below	28°34'06.5"S 17°39'21.0"E	Illite, microcline, albite, quartz, muscovite	see Sheet 2	see Sheet 3	0.4	2
3	TS-3	Karasburg (Nam)	1 m below	28°34'06.5"S 17°39'21.0"E	Illite, albite, quartz, muscovite, phengite	see Sheet 2	see Sheet 3	0.37	3
4	TS-4	Karasburg (Nam)	2.5 m below	28°34'06.5"S 17°39'21.0"E	not analyzed	see Sheet 2	XRD data corrupted	not analyzed	4
5	TS-5	Karasburg (Nam)	5 m above	28°32'34.2"S 17°41'12.6"E	not analyzed	see Sheet 2	not analyzed	not analyzed	5
6	TS-6	Laingsburg (SA)	N/A (no sills in the region)	33°10'57.9"S 20°49'03.4"E	Illite, chlorite*, muscovite, albite, quartz	see Sheet 2	XRD data corrupted	0.37	6
7	TS-7	Laingsburg (SA)	N/A (no sills in the region)	33°12'12.6"S 20°37'41.2"E	not analyzed	see Sheet 2	XRD data corrupted	not analyzed	7
8	TS-8	Laingsburg (SA)	N/A (no sills in the region)	30°56'40.4"S 19°25'48.9"E	Illite, chlorite*, muscovite, albite, quartz	see Sheet 2	XRD data corrupted	0.37	8
10	TS-10	Loeriesfontein (SA)	>30 m	30°56'29.8"S 19°25'40.3"E	not analyzed	see Sheet 2	not analyzed	0.71	10
11	TS-11	Loeriesfontein (SA)	>30 m	30°56'48.7"S 19°25'39.8"E	Illite, chlorite*, muscovite, albite, quartz	see Sheet 2	see Sheet 3	0.69	11
12		Loeriesfontein (SA)	>30 m	30°56'48.7"S 19°25'39.8"E	not analyzed	not analyzed	not analyzed	not analyzed	12
13	TS-13	Calvinia (SA)	15 m below	31°10'57.1"S 19°41' 07.6"E	not analyzed	see Sheet 2	see Sheet 3	not analyzed	13
14	TS-14	Loeriesfontein (SA)	>30 m	30°56'40.4"S 19°25'48.9"E	not analyzed	see Sheet 2	see Sheet 3	0.59	14
15	TS-15	Calvinia (SA)	20 m below	31°10'57.1"S 19°41'07.6"E	not analyzed	see Sheet 2	see Sheet 3	0.61	15
16	TS-16	Calvinia (SA)	3 m below	31°16'00.3"S 19°42'55.6"E	Minehillite, muscovite, 2M1, albite, chlorite, quartz	see Sheet 2	see Sheet 3	0.41	16
17 (1)	TS -17 (1)	Calvinia (SA)	3 m above lower sill	31°16'02.0"S 19°42'59.2"E	Illite, phengite, calcite**, albite, muscovite, chlorite, quartz	see Sheet 2	see Sheet 3	0.35	17 (1)
17 (2)	These samples were taken for reproducibility, within 1 m from one another	Calvinia (SA)	3 m above lower sill	31°16'02.0"S 19°42'59.2"E	not analyzed	not analyzed	not analyzed	not analyzed	17 (2)
17 (3)		Calvinia (SA)	3.3 m above lower sill	31°16'02.0"S 19°42'59.2"E	Illite, phengite, calcite**, albite, muscovite, chlorite, quartz	not analyzed	not analyzed	0.35	17 (3)

* detrital phyllosilicate ** possible hydrothermal alteration mineral

Appendix table 2. XRF results: Whitehill Formation samples (*continued*)

	Karasburg Basin, Namibia						Calvinia, South Africa			Loeriesfontein, South Africa			Laingsburg, South Africa		
Sample	TS-4	TS-1	TS-2	TS-3	TS-5	TS-15	TS-13	TS-16	TS-17	TS-10	TS-11	TS-14	TS-6	TS-7	TS-8
Distance (m) relative to sill	-2.5	-2.0	-1.5	-1.0	+5.0	-20.0	-15.0	+3.0	-3.0	+30	+30	+30	+30	+30	+30
Major Oxides in wt %															
SiO_2	72.350	59.821	67.063	62.479	71.368	47.552	63.157	64.997	69.012	61.832	49.156	65.848	63.531	68.470	66.925
TiO_2	0.754	0.635	0.506	0.624	0.660	0.601	0.620	0.739	0.567	0.518	0.514	0.702	0.677	0.520	0.765
Al_2O_3	13.186	18.675	17.033	18.868	14.447	14.579	16.144	15.783	14.714	13.223	13.781	15.276	16.100	15.013	13.334
Fe_2O_3	0.589	7.976	5.283	6.139	0.449	4.609	3.271	0.566	4.753	1.648	2.402	1.295	1.516	3.417	0.848
MnO			0.014					0.125			0.033			0.112	0.014
0.017			0.011					0.014			0.217			0.011	0.011
0.010			0.037					0.049			0.011				
MgO	0.469	2.693	1.832	2.445	0.416	1.528	0.822	1.024	1.151	1.078	0.778	0.909	1.118	1.125	0.659
CaO	0.524	0.989	0.262	0.343	0.569	0.631	0.101	0.149	1.348	0.091	0.059	0.157	0.223	0.402	0.344
Na_2O	2.058	2.819	1.582	1.425	2.478	1.211	2.429	1.802	1.964	1.614	1.543	1.500	1.681	2.121	1.651
K_2O	3.254	2.418	3.216	3.703	3.450	2.623	3.532	3.675	2.735	2.286	2.476	2.807	2.932	2.797	2.707
P_2O_5	0.123	0.552	0.096	0.133	0.124	0.517	0.152	0.062	0.535	0.126	0.250	0.056	0.066	0.140	0.060
LOI	6.433	3.108	2.921	3.333	5.170	25.386	9.524	10.732	2.258	17.415	28.156	10.947	11.683	5.498	11.867
Total	99.754	99.810	99.827	99.605	99.146	99.254	99.761	99.543	99.253	99.842	99.125	99.507	99.563	99.552	99.170
TOC	0.27	1.86	1.57	0.11	4.04	15.25	3.30	8.24	0.30	14.05	16.60	7.01	7.33	1.69	9.21
Traces in ppm															
Mo	2.1	<0.5	<0.5	<0.5	<0.5	25.0	<0.5	18.1	<0.5	8.6	5.9	1.6	3.2	<0.5	2.7
Nb	17.3	13.0	13.7	15.4	17.9	13.5	16.4	15.5	13.6	14.3	10.9	14.8	15.3	13.7	15.1
Zr	182.9	159.7	160.3	174.3	173.6	146.7	161.5	158.0	163.3	128.1	135.1	147.5	152.2	157.0	153.8
Y	31.2	44.0	34.5	36.5	44.0	51.4	32.1	27.6	36.5	27.0	24.9	30.9	42.3	33.9	26.9
Sr	206.6	145.6	82.0	126.5	266.2	157.6	110.1	78.3	262.1	126.2	101.7	70.0	70.9	98.0	60.6
Rb	136.7	116.8	176.3	205.3	154.5	135.6	180.3	175.9	134.4	127.1	140.1	157.7	154.4	143.2	129.9
U	1.7	1.7	<1.5	<1.5	2.2	5.1	<1.5	<1.5	2.3	<1.5	<1.5	<1.5	<1.5	<1.5	<1.5
Th	20.4	16.9	13.7	16.1	15.6	17.8	16.0	17.5	13.1	12.9	13.6	12.8	9.4	12.9	8.6
Pb	47.9	81.0	36.2	12.1	49.6	52.9	33.5	31.4	19.5	61.4	37.2	31.9	24.7	11.1	20.8
Zn	9.1	83.6	96.8	42.8	7.2	17.7	47.9	14.9	83.1	32.6	24.8	13.0	31.9	165.0	11.5
Cu	4.3	3.1	43.8	48.0	11.8	73.5	33.9	22.3	59.9	24.3	35.8	30.6	19.4	12.9	7.6
Ni	<1.8	19.7	17.4	11.8	<1.8	16.2	9.3	5.3	17.4	9.1	11.2	2.3	18.3	26.1	4.8
Co	<2.2	17.4	7.5	9.2	<2.2	<2.2	<2.2	<2.2	5.8	<2.2	<2.2	<2.2	5.1	6.4	<2.2
Mn	65.3	1155.6	229.8	962.7	28.3	104.8	39.3	74.1	950.6	56.2	65.0	28.9	362.0	363.5	42.4
Cr	121.7	48.6	51.4	52.5	48.9	1106.6	44.7	1176.6	55.7	52.8	88.0	70.9	60.3	43.8	91.0
V	125.7	119.3	109.9	130.1	124.4	167.2	105.9	111.9	95.0	90.4	151.8	100.5	99.6	68.1	82.6
Sc	21.6	16.1	15.5	17.9	15.7	22.5	14.0	15.8	14.8	13.2	17.9	14.0	15.4	10.4	11.9
Ba	702.5	515.4	609.1	534.1	805.7	956.1	931.8	774.5	677.7	559.9	911.1	605.9	626.8	555.7	682.8
S	2857.3	1.7	45.4	1.3	505.7	5495.5	3237.5	2692.4	13.0	6865.5	3626.6	2274.0	5358.8	133.8	4982.4

* detrital phyllosilicate ** possible hydrothermal alteration mineral

Appendix Figure 1. XRD results: Whitehill Formation samples (*continued*)

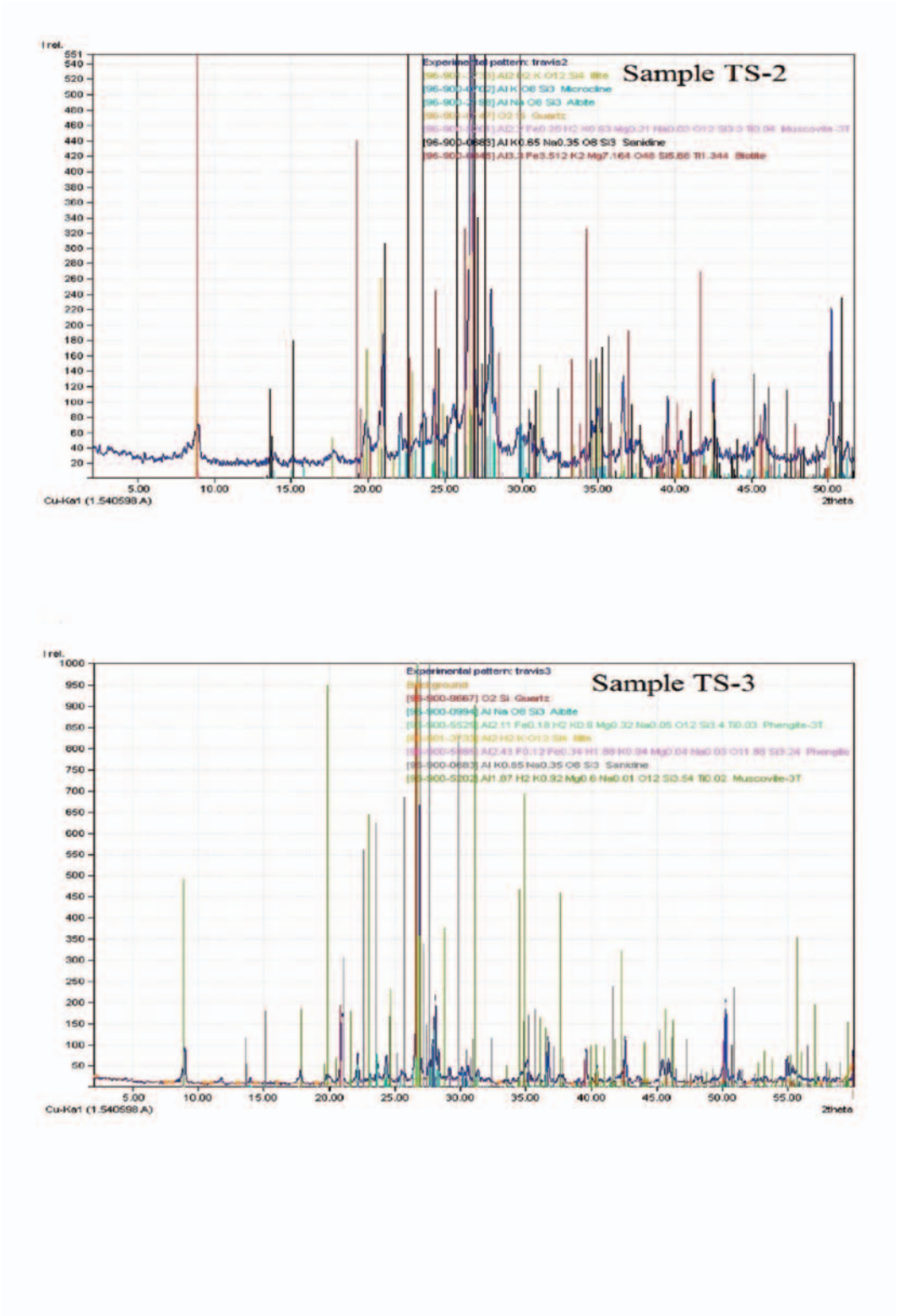

Appendix Figure 1. XRD results: Whitehill Formation samples (*continued*)

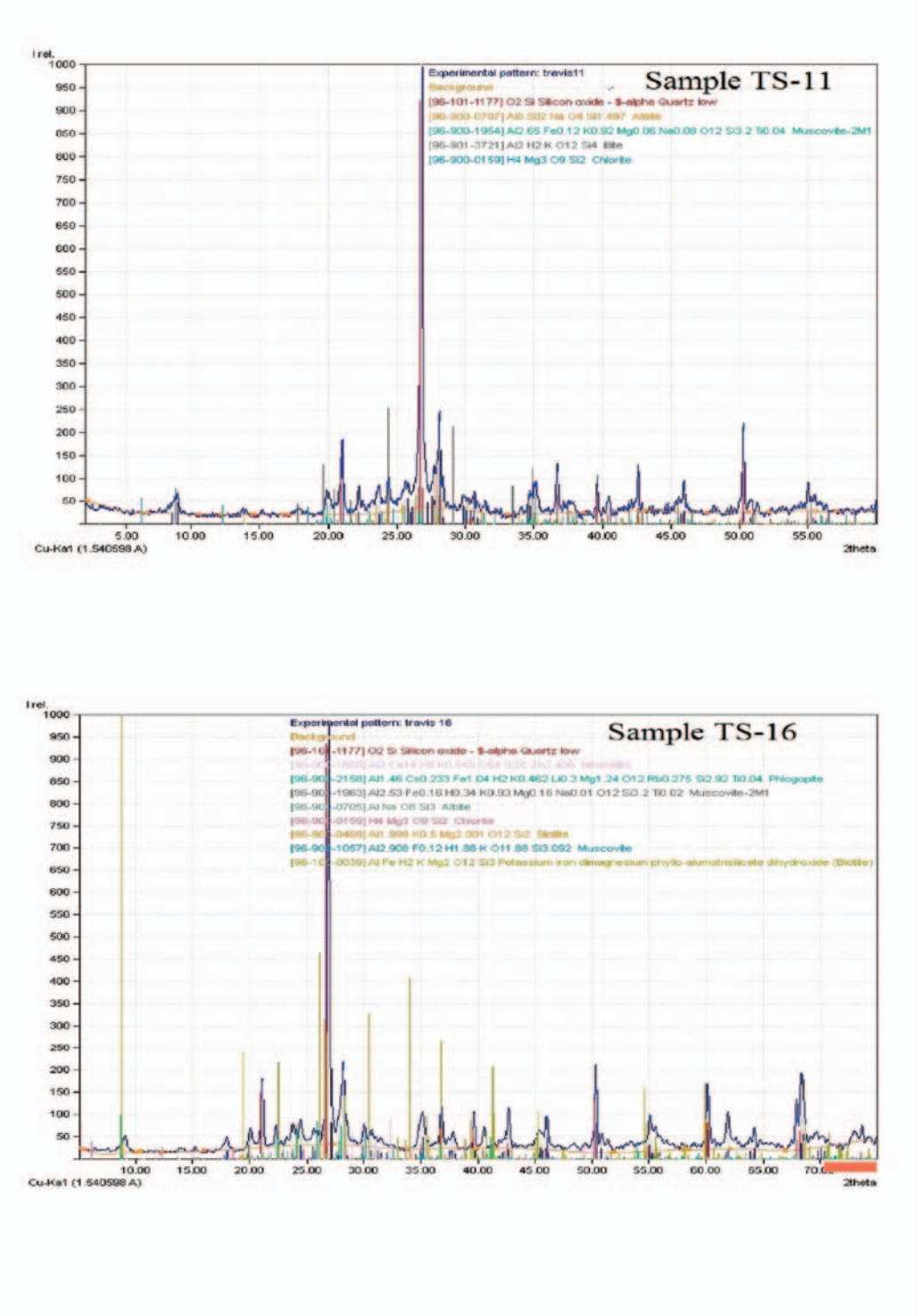

Appendix Figure 1. XRD results: Whitehill Formation samples (*continued*)